RESEARCH ON THE OPTICAL STATE OF THE ATMOSPHERE

by

Michael McClintock
Alden McLellan
Leaf Turner

A Report to

The Environmental Protection Agency

on research conducted between

August 1, 1971 and June 1, 1972

EPA-R3-72-027

Contract No. 68-02-0337

Principal Investigator: Michael McClintock

The Space Science and Engineering Center
The University of Wisconsin
1225 West Dayton Street
Madison, Wisconsin 53706

November 30, 1972

CONTENTS

I — INTRODUCTION

This is the third report to the Environmental Protection Agency in a series that deals with research on the feasibility of using satellite-based instruments to detect atmospheric pollution. The first report was titled "Studies on Techniques for Satellite Surveillance of Global Atmospheric Pollution," and was submitted to the National Air Pollution Control Administration (since incorporated into the Environmental Protection Agency) in September, 1970. The second report was titled, "Satellite Measurement of Spectral Turbidity and Albedo, and their Rates of Change," and was submitted to the Environmental Protection Agency in July, 1971. Where discussions in the present report depend on the earlier work, an appropriate reference is made rather than repeating the prior material.

The report investigates the possibility of climatic change from the radiative interference from dust and clouds in the atmosphere, provides an example of satellite detection of large-scale atmospheric pollution and a laboratory experiment on the non-Lambertian radiative reflection properties of urban areas, and presents a theoretical treatment of electromagnetic scattering from randomly oriented anisotropic particles with the intent of obtaining information about their shape.

II — CLIMATIC CHANGE FROM DUST AND CLOUDS

If there is disagreement among workers in the field of global air pollution as to the extent that man's activities may be responsible for climatic change, there seems to be a consensus that the problem must be looked into. The possibility is well founded that whether of man-made or natural origin, changes in atmospheric composition may lead to changes in the radiative energy balance of the earth, and hence to climatic variation.

A series of papers have dealt with two of the important variable constituents of the atmosphere: carbon dioxide and particulate matter (dust). In 1956, Plass [1] directed attention to the greenhouse effect of CO_2, and it was widely accepted that the increased CO_2 content of the atmosphere caused by greater combustion was responsible for the gradual increase in mean surface temperature.

But the observation documented most recently by Mitchell [2], that the mean temperature appeared to be decreasing since some time in the 1940's, seemed to call for an appropriate effect which exceeded the greenhouse effect of CO_2. A phenomenon with a time constant of the same order as the observed CO_2 increase was necessary, and McCormick and Ludwig [3] proposed an increase in airborne dust to account for the temperature decrease. Charlson and Pilat [4] pointed out that the optical properties of the dust are important in determining the sign of the temperature change, and Lettau and Lettau [5], and later Atwater [6] showed how the reflectivity of the earth's surface also enters into determining the change in albedo when dust is present in the atmosphere. More recently Rasool and Schneider [7] have performed a more sophisticated analysis and have demonstrated, consistently with Atwater, that if the surface reflectivity is low and particles are small, the initial effect of increasing dust should be to cool the earth. In a later analysis by Mitchell [8], however, the predominant effect of a tropospheric aerosol near the surface is shown to be very likely one of warming rather than cooling.

Although it is not always stated explicitly, all these workers must surely realize that the part of the problem they have addressed may not be the most important part from the standpoint of climatic change. Radiative transfer modification by CO_2 and dust may be only the first step in a series of coupled processes by which the planetary energy balance undergoes a change. If a change in atmospheric dust results in a change in mean cloudiness, for example, as recent urban climatic studies suggest [9], this could be the determining factor in a change of the planetary albedo, considering the high reflectivity of many clouds as seen from the top. Clouds also usually behave as black bodies in the infrared, greatly altering the radiative characteristics of the part of the atmosphere which they occupy. Thus, even if dust only moderately influences mean cloudiness, the optical effects of changes in cloudiness are probably large enough that the dust-cloud interaction cannot be overlooked as a possible determinant of climatic change. Among recent authors who have dealt with this possibility in climatic terms are Mitchell [8]

and Robinson [10]. In fact, if one grants that the most important variable quantities in the earth's atmosphere from the standpoint of the planetary radiation balance are probably water vapor, cloud, dust, CO_2, and O_3, and that a change in the amount of one of them may produce changes in others, it seems clear that an understanding of the problem has just begun.

We wish to indicate in this section that the interaction between dust and clouds need not be large to be significant in affecting the temperature near the earth's surface. We also have constructed a simplified mathematical model in an attempt to demonstrate one possible functional dependence of mean cloudiness on particulate matter in the atmosphere.

Since Chagnon's controversial study of precipitation patterns at LaPorte, Indiana [11], attention has been directed toward the possibility that air pollution is acting as a seeding agent in clouds downwind of major industrial centers. Evidence of this is not clear-cut because precipitation is also induced by the heat island of the city as well as by prominent geographic features (LaPorte, for example, is situated near Lake Michigan). On the other hand, there is also evidence that cloud condensation nuclei may sometimes be so numerous that overseeding of clouds occurs [12]. Overseeding encourages the growth and thickening of clouds and thwarts their tendency to dissipate through precipitation. Thickening of cloud cover can also occur by another mechanism. Recent studies indicate that the effluent of steel mills [13], and lead from automobiles combined with traces of iodine in city air [14] may serve as excellent ice nucleation sites in clouds. Large quantities of latent heat released by ice formation can cause the explosive growth of the cloud [9]. This is an important consequence, for it is well known that cloud albedo, transmissivity and emissivity are sensitive to cloud thickness.

Of course, atmospheric dust itself has the potential to dramatically alter climate if it exists in sufficient quantities. On the mesoscale, Bryson and Baerreis [16] have found that the presence of heavy concentrations of dust in the atmosphere over the Rajasthan Desert of northwest India increases the diabatic cooling rate of the midtroposphere by 30 to 50%. This leads to an increased subsidence rate which promotes the continued aridity of the region, in spite of the fact that sufficient moisture exists for much more frequent precipitation. On the global scale, the numerical model of Rasool and Schneider [7] provides a clue to the radiative effects of increasing background turbidity. The model predicts that a four-fold (400%) increase in dust would lead to a 3.5° K decrease in mean global temperature. A decrease of this magnitude is probably sufficient to increase the long-term ice coverage of land masses significantly [17].

The Effect of Clouds on Surface Temperature

As a first step in comparing the relative effect of clouds and dust on climate, an attempt was made to determine the amount of variation in mean cloudiness necessary to cause a decrease in surface temperature of

3.5°, so that this could be compared with the result of Rasool and Schneider. Work by Lettau and Lettau [5] and Manabe and Wetherald [18] provided the information necessary to perform two independent calculations of this sort.

Lettau and Lettau make use of statistical data obtained by Haurwitz [19] which relates radiation to fractional cloudiness, and a study by Neiburger [20] based on measurements of shortwave radiation fluxes for varying stratus cloud thickness. In the Lettau model cloud type was substituted for cloud thickness. The three parameters of albedo, absorption and scattering were adjusted so that increases in mean cloudiness reproduced Haurwitz's data. The Lettau paper includes the calculated changes in radiation flux for a stepwise increase in fractional cloudiness (from 0 to 1 in increments of one-third) for both cirrus and stratus over representative city, desert and prairie surfaces (Kew, England; Pampa de La Joya, Peru; and O'Neill, Nebraska, respectively). The data in this paper were used in our calculation of surface temperature which follows.

In the notation of Lettau, the fraction of incoming radiation that is absorbed at the surface is $(1-a)G^*$ where a is the surface albedo and G^* is the fraction of incident radiation. For steady-state conditions

$$S_0(1-a)G^* = \varepsilon\sigma T^4 + Q \qquad (1)$$

where S_0 is the solar constant, $\varepsilon\sigma T^4$ is the radiative heat transfer, and Q the combined conductive and convective heat transfer from the surface. T was then allowed to vary from a value of $T_1 = 290°K$ (chosen as a typical average daylight temperature over land) to $T_2 = 286.5°K$, a ΔT of $-3.5°K$. As a first approximation, it was assumed that Q did not vary, an assumption open to obvious question but one which is not likely to change the result by an order of magnitude. Thus

$$S_0(1-a)(G_1^* - G_2^*) = \varepsilon\sigma(T_1^4 - T_2^4) = \varepsilon\sigma(T_1^4 - (T_1-\Delta T)^4). \qquad (2)$$

ε, the emissivity, was taken to be unity and the right side of the expression was expanded about T_1 to obtain:

$$(1-a)(G_1^* - G_2^*) = 4\sigma T_1^3 \Delta T/S_0 \simeq 0.014 \ . \qquad (3)$$

By linear interpolation between the values of fractional cloudiness listed in Table 8 of Lettau [5], it was possible to determine how much increase in cloudiness causes a ΔT of $-3.5°K$. The results appear below:

Cloud Type	Kew	La Joya	O'Neill
Cirrus	+ 8.6%	+ 11.9%	+ 11.3%
Stratus	+ 3.0%	+ 3.2%	+ 3.2%

Comparing these results with the 400% change in dust content of the atmosphere which Rasool and Schneider calculated for the same change of temperature, one sees the considerably greater effectiveness of clouds. This is not a particularly surprising result, of course, but it does provide the opportunity for quantitative comparison.

The same comparison can be obtained by another method from Manabe and Wetherald's [18] numerical model of atmospheric radiation for a fixed distribution of relative humidity. One part of the model computations involved a series of radiative and convective thermal equilibrium calculations for varying distributions of cloudiness at low, middle and high altitudes. The reflectivity of solar radiation was assumed to be 20% for cirrus clouds, 48% for middle clouds, and 69% for low clouds, based on observations by Haurwitz. Low and middle clouds were treated as full black bodies, cirrus as half-black. The average fraction of cloud cover was taken to be 0.218 for cirrus, 0.072 for middle, and 0.306 for low cloud. The fraction of each type of cloud was then varied from 0 to 1 while the other two types were held fixed at their average fractional values, and the resulting surface temperatures were calculated.

If it is assumed that atmospheric dust effectively increases low and middle clouds only, the fractional change of each type required to lower surface temperature by 3.5°K can be readily calculated from the results of Manabe (Table 9 [18]). It is found that an increase of 4.5% of low cloud or 9.2% of middle cloud is sufficient to lower surface temperature by this amount. These estimates agree well with those derived independently from Lettau's climatonomy model. The agreement is still more impressive when it is recalled that Lettau's results are based largely on observational data, while Manabe and Wetherald have used a purely analytical model.

Dividing the 400% change in dust content required for a 3.5°K temperature change (Rasool and Schneider) by the percentage change in cloudiness required for the same effect, we see that low and middle clouds are perhaps some 30 to 130 times more effective than dust in changing the surface temperature.

Interaction Between Dust and Clouds

Among the activities recommended by the participants of the recent SMIC conference on inadvertent climate modification [21] was the use of simplified parameterized climatic models in order to gain insight into some of the basic factors of climate and climate change. It is therefore desirable to construct a simplified model which incorporates those features of cloud formation and depletion appropriate to evaluate changes in mean cloudiness that may arise from a gradual flux of particles from the stratosphere to the troposphere. Such a model might be thought to describe, for example, the gradual fallout over several years of stratospheric dust from a violent volcanic eruption. If all other meteorological processes are allowed to operate without modification, the minor perturbation of stratospheric fallout would lead to the following rate equation for the fractional cloudiness in a given area:

$$\frac{df}{dt} = K_1H + K_2f + K_3\phi f \qquad (4)$$

where df/dt is the rate of change of fractional cloudiness, $0 \leq f \leq 1$. H is the rate of latent heat energy due to surface evaporation and is thus proportional to the rate or evaporation of moisture, ϕ is the flux of atmospheric particles which play the role of cloud condensation nuclei, and the coefficients K_1, K_2, K_3 are proportionality constants which contain the physics of cloud formation and depletion. This basic rate equation for the change of cloud cover over an area is an expression designed to illustrate the effect of gradual particulate fallout from stratosphere to troposphere by singling out this process in the last term of the equation. In the other terms we are interested in establishing only a physically reasonable dependence on other variables which enter the energy balance equations set forth later for a two-layer atmospheric model. Thus K_1H represents the physically reasonable assumption that the rate of cloud formation over a sufficiently large area is, on the average, proportional to the rate of evaporation of moisture from the surface and is thus proportional to H. The quantity K_1 represents the mean atmospheric conditions which contribute to cloud formation over the area. The term K_2f likewise represents the physically reasonable assumption that the rate of cloud dissipation over a sufficiently large area is, on the average, proportional to the existing cloudiness, with the constant of proportionality K_2 containing the mean atmospheric conditions which contribute to cloud dissipation over the area. To see this, one imagines the sky over the area to be divided into smaller units of area, N in total, of which n subunits may be considered covered by clouds. Then since each of the subunits is independent of the others, to first order, it is clear that

$$\frac{dn}{dt} = kn \qquad (5)$$

where k is a constant. Also, since $f = n/N$, we have immediately the dissipative term in Eq. (4):

$$\frac{df}{dt} = kf \ . \qquad (6)$$

The same logic supports the f-dependence of the term expressing the effect of particulate flux from the stratosphere into the troposphere. In addition, we suppose this term to be linearly dependent on the particle flux, ϕ, in the range of particle fluxes appropriate to long-term fallout from explosive volcanic eruptions. We will refer to K_3 as the "seeding interaction coefficient," although we do not insist that its algebraic sign be negative for all areas of the earth which one might consider. In fact, the magnitude and sign of K_3 depends upon local conditions. If the number and size distribution of aerosol is such that seeding occurs, the resultant induced precipitation would presumably cause decreases in mean cloudiness. On the other hand, if the dust overseeds the clouds, increases in cloud cover and attendant decreases in precipitation may result. However, if the dust is so heavy that a pronounced increase in stagnation occurs (as in the Rajasthan), the dynamic condi-

tions will not be favorable for cloud formation and the sign of the interaction will once again be negative. This suggests the existence of threshold levels of dust concentration which serve as lines of demarcation between the seeding, overseeding and stagnation regimes.

The SMIC report summarizes what is known about the first two of these processes in terms that illustrate present uncertainties [21]:

> ...An increase in the number of cloud nuclei could lead to a decreased efficiency of rain formation, especially in regions where rain is formed predominantly in nonsupercooled clouds and where the air is naturally low in cloud nucleus content. If the water vapor input remained constant, an increase in cloud cover or cloud depth (or both) would result. Another possible effect of particle pollution works in the opposite sense: if giant soluble particles or effective ice nuclei are added inadvertently or otherwise by man's activities, then a possible stimulation of precipitation or cloud dissipation, accompanied by a reduction in cloud cover, could result. To sum up, it may be said that mechanisms exist whereby cloud cover may be increased by pollution. Mechanisms that are probably less important tend to decrease cloud cover.

Since at steady state $df/dt = 0$, Eq. (4) can be solved immediately for the steady state value of f, and, given the probability that $K_3\phi \ll K_2$, can be expressed in the form of a convenient approximation:

$$f = -\frac{K_1 H}{K_2 + K_3 \phi} = -\frac{K_1}{K_2} H\left(1 - \frac{K_3\phi}{K_2}\right). \tag{7}$$

Probably $K_3 > 0$, as we have discussed, and given that $K_2 < 0$, we see that an increase in ϕ implies an increase in f, as it should, if H does not change greatly with ϕ. Mathematically expressed, we note in passing that $\partial f/\partial\phi > 0$ if $\partial H/\partial\phi > 0$, as expected, since

$$\frac{\partial f}{\partial \phi} = \frac{K_1 H}{K_2^2} K_3 - \frac{K^1}{K_2}\left(1 - \frac{K_3\phi}{K_2}\right)\frac{\partial H}{\partial \phi}.$$

The rate of surface evaporation H is a function of the surface temperature of the earth T_E and may be expressed conveniently as

$$H = b(V_H)[p_{sat}(T_E) - p] \tag{8}$$

where $b(V_H)$ is a coefficient proportional to the mean horizontal winds V_H, $p_{sat}(T_E)$ is the (saturated) vapor pressure at temperature T_E, and p is the actual partial pressure of water vapor in the atmosphere at the surface. The vapor pressure of water as a function of temperature may be expressed in a form familiar for most liquids:

$$p_{sat}(T_E) = C \exp(-\frac{L}{RT_E}) \tag{9}$$

where C is a constant. Thus we have

$$H = b(V_H)[C \exp(-\frac{L}{RT_E}) - p] \ . \tag{10}$$

The surface temperature will depend on the fractional cloudiness since clouds modify both the visible and infrared radiative transfer of the atmosphere. If $T_E(f)$ is determined, $H(T_E)$ can be expressed as a function of f and Eq. (7) may then be solved to obtain f as a function of ϕ. This will provide some insight into the functional dependence of f upon stratospheric dust content.

In order to determine $T_E(f)$, a set of local energy balance equations for a two-layer atmosphere can be written:

Earth Surface: $$F_0(1-f\alpha) + [(1-f)a_T+f]\sigma T_T^4 + t_T(1-f)a_S\sigma T_S^4 = \sigma T_E^4 + H \tag{11}$$

Troposphere: $$[(1-f)a_T+f]\sigma T_E^4 + [(1-f)a_T+f]a_S\sigma T_S^4 + H = 2[(1-f)a_T+f]\sigma T_T^4 \tag{12}$$

Stratosphere: $$(1-f)t_Ta_S\sigma T_E^4 + [(1-f)a_T+f]a_S\sigma T_T^4 = 2a_S\sigma T_S^4 \tag{13}$$

where F_0 is the diurnally averaged local solar flux; T_E, T_T, and T_S are the temperatures of the earth, troposphere and stratosphere, respectively; a_T and t_T are the absorptivities and transmissivities of the troposphere, a_S the absorptivity of the stratosphere; α is the albedo of the clouds which occupy a fraction f of the sky; H is the rate of transfer of latent heat of evaporation from the surface, as before.

The above equations are based on a model subject to the following restrictions:

(i) The atmosphere is considered transparent to visible radiation;

(ii) For the longwave spectrum, the earth and clouds are assumed to be black, the atmosphere gray;

(iii) The tropospheric water vapor content is taken as constant, and no convective contact between the troposphere and stratosphere is provided for;

(iv) The clouds in the model have an effective albedo α, but do not absorb in the shortwave.

At first glance these restrictions may appear to be too unrealistic to be useful, but since the philosophy of the effort is to determine small *changes* in the steady-state value of cloudiness, brought about by a minor perturbation, errors in the description of the system itself tend to diminish in importance if observed steady-state data are used as the point of departure in the final quantitative evaluation.

Equations (11), (12) and (13) may be solved simultaneously for σT_E^4:

$$\sigma T_E^4 = \frac{F_0(4-a_S a_T) + [F_0(a_S a_T \alpha + a_S a_T - a_S - 4\alpha) + \frac{K_2+K_3\phi}{K_1}(2-a_S a_T - a_S t_T)]f}{[4-2a_T-a_S(1+2a_T t_T+2t_T^2)] + [a_S(-1+a_T+4a_T t_T-2t_T+4t_T^2)-2(1-a_T)]f}$$

$$+ \frac{[F_0 \alpha a_S(1-a_T) - \frac{K_2+K_3\phi}{K_1} a_S(1-a_T-t_T)]f^2}{+ [2a_S t_T(1-a_T-t_T)]f^2} . \qquad (14)$$

If longwave backscattering from dust and molecular constituents is neglected, then $a_T + t_T = 1$, and Eq. (14) simplifies somewhat. Furthermore, we can neglect terms in the product of small fractional quantities relative to terms of order unity or greater (i.e., terms in the product $a_S t_T$) to obtain an equation for σT_E^4 which is linear in f:

$$\sigma T_E^4 = \frac{F_0(4-a_S a_T) + [F_0 \alpha(a_S a_T - 4) + \frac{K_2+K_3\phi}{K_1}(2-a_S)]f}{(4-2a_T-a_S)} . \qquad (15)$$

The steady-state fractional cloudiness may then be expressed as

$$f = -\frac{K_1}{K_2+K_3\phi}\left\{b(V_H)\left[C \exp\left[-\frac{L}{R}\left(\frac{F_0(4-a_S a_T)+[F_0\alpha(a_S a_T-4)+\frac{K_2+K_3\phi}{K_1}(2-a_S)]f}{\sigma(4-2a_T-a_S)}\right)^{-\frac{1}{4}}\right]-p\right]\right\} . \qquad (16)$$

Because of the complexity of this equation, a graphical or numerical solution for $f(\phi)$ is called for. Values of ϕ appropriate to an explosive volcanic eruption might then be used to calculate corresponding values of f, provided mean values of the other parameters in Eq. (16) are known for the region of interest. Current climatological observations must be used to determine these parameters, with ϕ set equal to zero. The seeding interaction coefficient, K , may be estimated from cloud physics data extrapolated to the lighter particle fluxes appropriate for volcanic fallout from the stratosphere. Typical areas chosen might be, for example, a tropical ocean area, a midlatitude ocean area, a midlatitude continental area, a large desert area, an arctic area, etc. In this way one hopes to establish the variation of f with ϕ for

typical areas, and, by then using Eq. (15), find the corresponding variation in T_E.

Likely forms of the solution to this problem can be deduced from physical reasoning. They present a rich spectrum of possibilities. First, by simply looking at Eq. (15), one sees that if the predominant effect of a long term flux of particles from the stratosphere causes an increase in cloudiness f, then T_E will tend to be decreased by a larger (negative) first term in the square brackets simply because more sunlight is reflected by clouds. The second term in f is also negative (since K_2 is intrinsically negative and $|K_2| > |K_3\phi|$), so a larger value of of cloudiness will also decrease T_E because more heat is extracted from the surface by evaporation (recall Eq. (7)). The flux of infrared radiation from the surface is inhibited by absorption and reradiation of clouds and by the clear atmosphere; factors expressing this inhibition appear in terms containing a_S and a_T . This represents the part played by clouds and air in the real atmosphere in warming the earth, as opposed to their more obvious cooling effect in blocking incoming solar radiation.

One sees from Eq. (15) that the infrared energy radiated from the earth's surface is a linear function of the cloud cover, consistent with the calculations of Schneider (SMIC report, 1971, p. 119) which were based on a more complex atmosphere than that assumed here. Even without detailed numerical examination, it appears that the quadratic terms in the more precise Eq. (14) are small compared with the linear term, a fact which forms the basis for the simpler equation. This does not appear to be obvious from the assumptions made in constructing the model, but arises naturally in the solution of the descriptive equations.

Things, however, are actually more complex than this, since f itself depends on ϕ and atmospheric parameters as indicated in Eq. (16). This equation expresses quantitatively the way in which a change in cloudiness changes the surface temperature by allowing more solar absorption, which then changes the saturation water vapor pressure so that more clouds are made by additional evaporation. The full set of equations therefore expresses some of the important feedback mechanisms by which the radiative energy balance responds to an interaction between dust and clouds. One might wish for simpler expressions, but the natural system is complex, and any degree of fidelity to this system appears to demand a certain complexity of mathematical expression. Fortunately the computer holds out the hope that complexity of the necessary degree will not produce merely confusion and intractibility. Work along these lines is planned for the future.

Conclusions

1. An increase in carbon dioxide content of the earth's atmosphere acts to increase the surface temperature by inhibiting infrared radiation to space. An increase in dust content of the atmosphere modifies both visible and infrared radiative transfer in ways that depend sensitively on the optical properties of the dust, very likely producing a decrease in surface temperature except for very heavy industrial pollu-

tion and at high latitudes [21]. The present study calls attention to another mechanism by which atmospheric dust may influence climate: by interacting with atmospheric water vapor to modify cloud cover. Although this has been mentioned in the recent literature, no attempt at quantitative treatment appears to have been undertaken. We have shown here that a change in cloud cover is between approximately 30 and 130 times more effective (depending on cloud height and type) in causing a change in surface temperature than a change in dustiness by modification of the radiative transfer. The work of Rasool and Schneider [7] has shown that a change in dustiness of more than 100% is required to change the mean surface temperature 1° by modifying atmospheric radiative transfer. By comparison we find that a change in mean cloud cover of between approximately 1 - 4% will change the surface temperature this amount. Considering the mean planetary temperature change of approximately -0.3° since 1940, it would seem extremely desirable to have satellite measurements of cloud cover sensitive to long-term changes of 1%, at least over areas of greatest particle production if not the entire planet.

2. A simplified mathematical model based on energy balance, and incorporating a portion of the hydrological cycle in an *ad hoc* way, has been constructed to illustrate one mechanism by which the long-term fallout of dust from the stratosphere might bring about a change in mean cloudiness of an area. Graphical or numerical solution of the equations based on climatological observations is called for, but even a cursory analysis indicates the correct sign of the result, i.e., increased particle flux from the stratosphere to the troposphere (if it produces the probable effect of increased cloudiness) causes a decrease in surface temperature. This predicts a long-term cooling trend following large, explosive volcanic eruptions, and also corresponds to the sign of the mean global temperature changes noted since the 1940's. Lacking quantitative data, it is impossible to say whether this represents any more than just an interesting chance correlation, but at the present state of knowledge this must be said about the relation between almost all climatological observations and theories of climatic change.

References

1. Plass, G. N.: *Tellus*, 8, pp. 140 (1956).

2. Mitchell, J. M., Jr.: *Global Effects of Environmental Pollution*, Springer-Verlag/D. Reidel, New York, pp. 139 (1970).

3. McCormick, R. A. and Ludwig, J. H.: *Science*, 156, pp. 1358 (1967).

4. Charlson, R. J. and Pilat, M. J.: *J. Appl. Meteor.*, 8, pp. 1001 (1969).

5. Lettau, H. H. and Lettau, K.: *Tellus*, 21, pp. 208 (1969).

6. Atwater, M. A.: *Science*, 170, pp. 64 (1970).

7. Rasool, S. I. and Schneider, S. H.: *Science*, pp. 173 (1971).

8. Mitchell, J. M.: *J. Appl. Meteor.*, 10, pp. 703 (1971).

9. See, for example, Peterson, J. T.: "The Climate of Cities," NAPCA Publication No. AP-59, Environmental Protection Agency (1969).

10. Robinson, G. D.: "Long Term Effects of Air Pollution—A Survey," The Center for the Environment and Man, Publication CEM 4029-400 (1970).

11. Chagnon, S. A., Jr.: "The LaPorte Weather Anomaly—Fact or Fiction?" *Bull. Amer. Meteor. Soc.*, 49, pp. 4-11 (1968).

12. Warner, J.: "A Reduction in Rainfall with Smoke from Sugarcane Fires—An Inadvertent Weather Modification," *J. Appl. Meteor.*, 7, pp. 247-251 (1968).

13. Noblis, P. V., Radke, L. F., and Shumway, S. E.: "Cloud Condensation Nuclei from Industrial Sources and Their Apparent Influence on Precipitation in Washington State," *J. Atmos. Sci.*, 27, pp. 81-89 (1970).

14. Schaefer, V. J.: *Global Effects of Environmental Pollution*, op. cit., pp. 158.

15. Peterson, J. T. and Bryson, R. A.: Proceedings of the First National Conference on Weather Modification, Albany, New York (1968).

16. Bryson, R. A. and Baerreis, D. A.: *Bull. Amer. Meteor. Soc.*, 48, p. 3.

17. We are indebted to Dr. John Kutzbach of the University of Wisconsin Center for Climatic Research for pointing out to us that climatologists, in a manner of speaking, regard our present era as an ice age. Paleographic records indicate that Greenland and Antarctica, presently ice-covered, have been so for less than 0.1% of the time over which such records extend.

18. Manabe, S. and Wetherald, R. T.: "Thermal Equilibrium of the Atmosphere with a Given Distribution of Relative Humidity," *J. Atmos. Sci.*, 24, pp. 241-259 (1967).

19. Haurwitz, B.: "Daytime Radiation at Blue Hill Observatory in 1933," *Harvard Meteor. Studies No. 1* (1934).

20. Neiburger, M.: "Reflection, Absorption and Transmission of Insolation by Stratus Clouds," *J. Meteor.*, 6, pp. 98-104 (1949).

21. *Inadvertent Climate Modification—Report of the Study of Man's Impact on Climate (SMIC)*, M.I.T. Press, Cambridge, Mass. (1971).

III — REMOTE SENSING OF GLOBAL ATMOSPHERIC POLLUTION

1. Introduction

The origins of atmospheric particulates comprise a diverse group of sources both natural and man-made, and the particulates vary over a wide range of sizes, shapes, densities and chemical compositions. Large-scale natural pollution from windswept arid regions, aerosols, meteoric dust and volcanic activity contribute to the particulate loading of the atmosphere as well as man's contribution by the combustion of fuels, incineration of waste materials, and industrial process losses. Of man's total quantity of atmospheric pollutants, particulates make up only 10%. However, because of their widely varying economic and biological effects, man-made particulates are an enormous problem (Scorer, 1968; Wolkonsky, 1969). Natural atmospheric particulate matter, on the other hand, can cause local problems (intense dust and sand storms), but these phenomena will, in general, cover a much larger region and have a much stronger influence on climate.

In a discussion on the detection and surveillance of atmospheric pollution by remote sensing, one must first define not only the optical properties of the pollution but also the spatial dimensions and the frequencies of measurement. A knowledge of these objectives is necessarily inherent in the consideration of what instrumentation is to be used. It is the purpose of this paper to give a brief description of the most important types of pollutants in the earth's atmosphere and their foremost optical properties, as well as the measurements that have been performed. For convenience, the relative scales of measurement have been divided into three sections. The first section deals with spatial dimensions on the global scale and time domains on the order of years; the second section considers active remote sensing systems for very short time intervals (less than a second); and the third section covers the more popular passive systems used primarily for intermediate times and spatial dimensions.

2. Climatic Radiation Changes

It has been in the interests of physical climatologists to investigate the history of the earth's energy balance and, in particular, the role played by the atmosphere. A number of remote sensing instruments were developed in the nineteenth century in order to record the variations in sunlight due to atmospheric phenomena (Middleton, 1969). See Figure 1. These early sunshine recorders primarily made use of photochemical changes and thermal effects for the conversion of solar radiation energy. Even though these instruments were more of an attempt to quantify human well-being than a serious contribution to meteorological theory, they did serve as the forerunners of modern radiometers and pyranometers. See Figure 2.

Information on atmospheric radiation during this century is often obtained from radiation observation records kept over decades by both astronomers and meteorologists. Data from one of the oldest remote sensing optical instruments—the telescope—are presently being used to determine

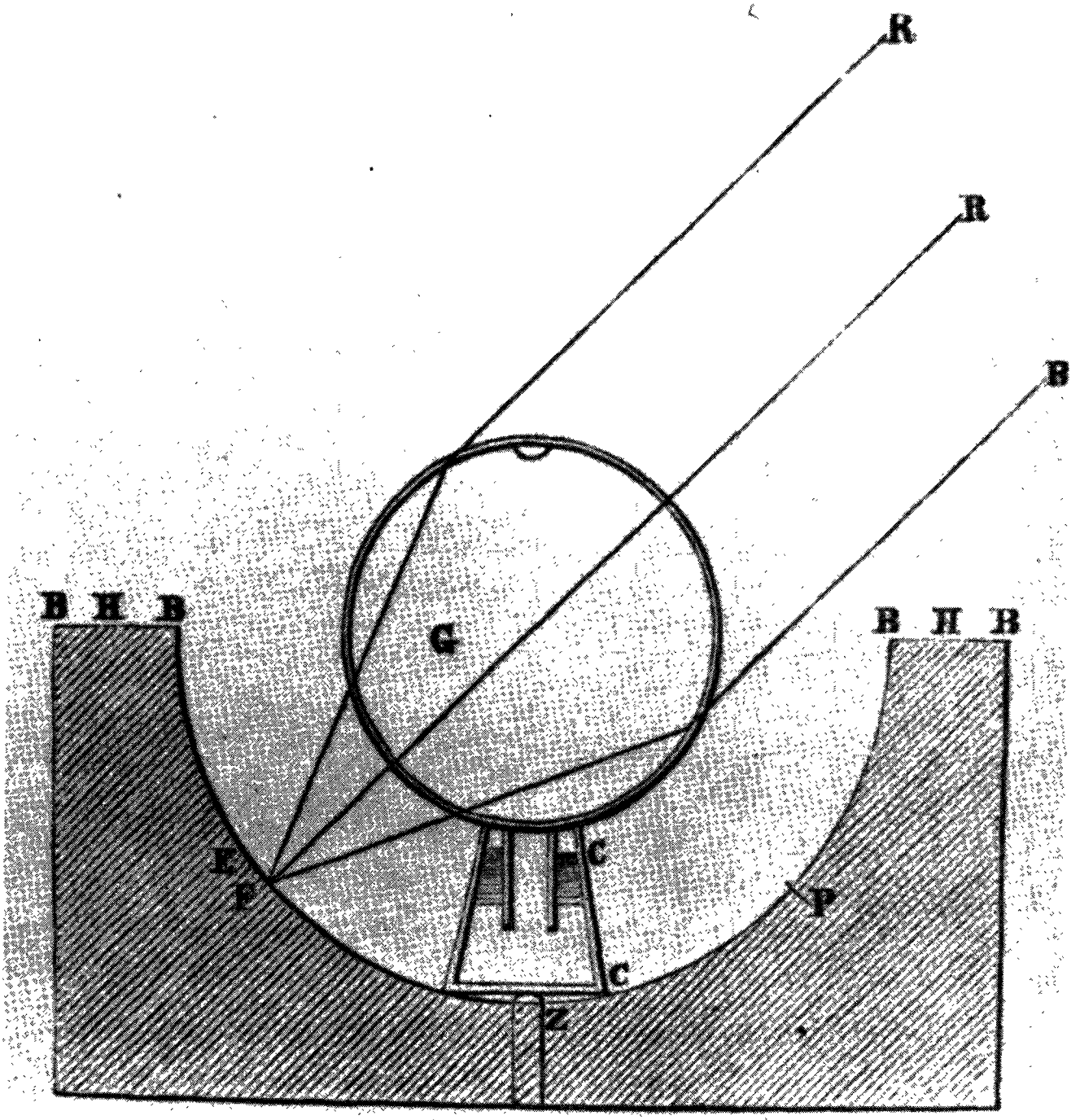

Figure 1. Nineteenth Century diagram of early sunshine recorders. Note that refraction takes place upon entering the sphere, but the draftsman neglected the refraction of light rays upon their exit.

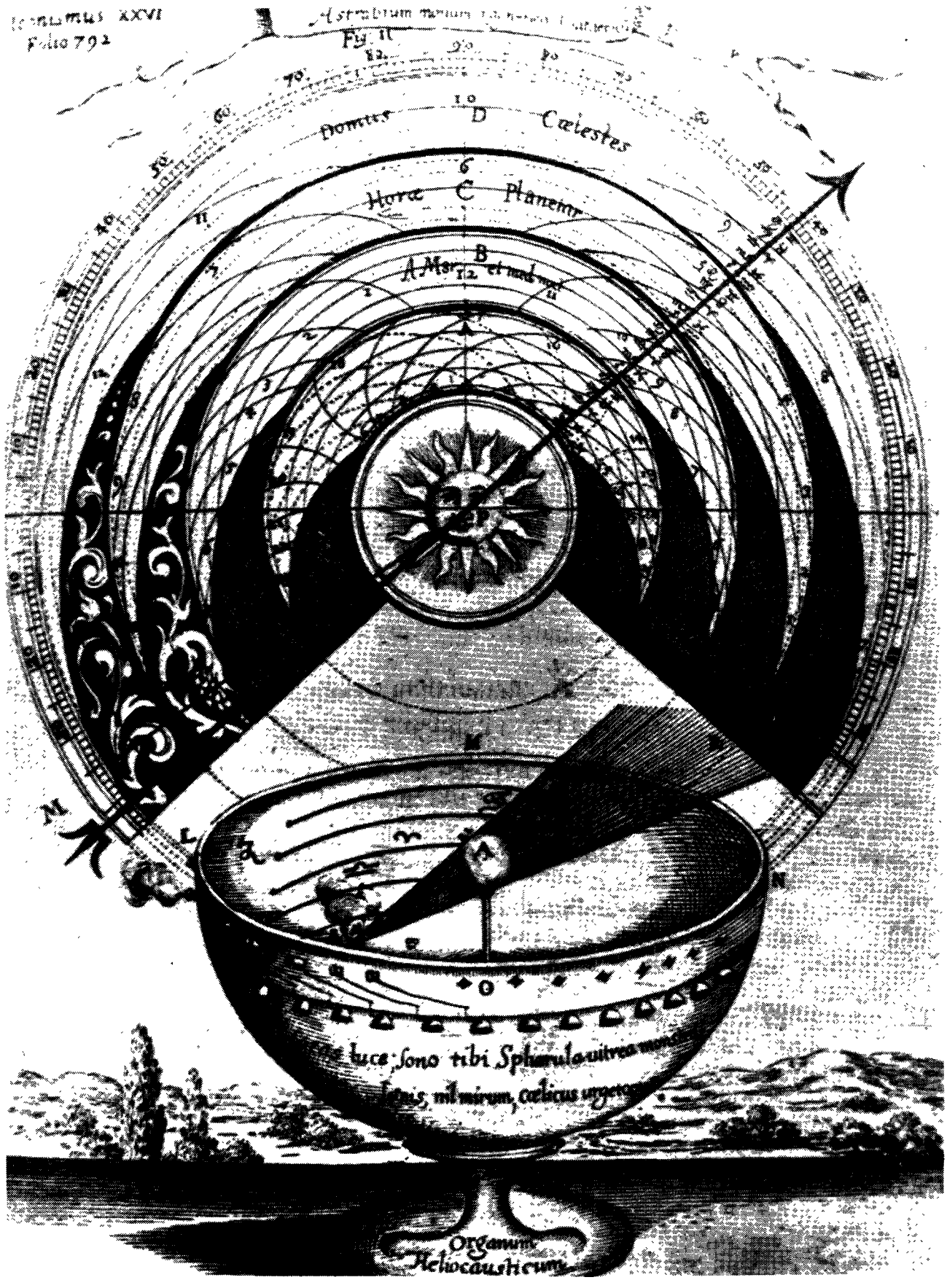

Figure 2. A crystal ball or a spherical flask full of liquid, placed centrally in a wooden hemispherical shell so that the sun's rays will burn a groove throughout the day. The depth of the groove was supposed to be related to the amount of sunlight. This idea was proposed as early as 1646.

atmospheric turbidity variation over the past century. A series of normalized photographic plates of the same sky area taken over a period of time can give an indication of the turbidity variation.

For the most part, climatologists have relied on a network of sampling stations for data on the gaseous pollutants of the atmosphere. To obtain information on the electromagnetic radiation reaching the earth's surface, a network of pyranometric ground stations measures the visible and near infrared radiation from the sun and sky. There are about 100 of these stations in the continental United States that use the Eppley pyranometer. Most of them have been in operation since the early 1950's. The pyranometer's 180° receiving surface has essentially two sensing elements under a glass hemisphere, one blackened to absorb a large proportion of the incident radiation, and the other coated white to reflect the visible radiation. If we assume, for simplicity, that the black element absorbs all incident radiation and the white element absorbs only the infrared radiation, then we have the energy equation for each element:

$$\begin{aligned} \text{(black)} \quad & Q + \sigma T_{glass}^4 = S_{black} + \sigma T_{black}^4 \\ \text{(white)} \quad & \sigma T_{glass}^4 = S_{white} + \sigma T_{white}^4 \end{aligned} \tag{1}$$

where Q is the shortwave solar radiation plus the shortwave diffuse sky radiation, σ is the Stefan-Boltzmann constant, S is the storage rate, and T is the temperature. We have assumed the infrared emissivity of the glass cover to be 1.0. Since the storage rate is a function of the physical and thermal properties of the sensor, and is proportional as well to its surface temperature, we have from Eqs. (1):

$$Q = k(T_{black} - T_{white}) \tag{2}$$

where the constant k is a function of the physical properties and is only weakly dependent on the temperature of the sensor. The temperature difference between the two ring sensors is measured with a large number of thermojunctions. The Eppley pyranometer has 16 to 50 thermojunctions (depending on the required precision) which are in thermal contact with the lower surface of two thin, flat concentric silver sensor rings. The assembly is enclosed in a blown spherical glass dome that is filled with dry air. This limits the radiation to wavelengths between 0.3 - 0.4μ to 3.0 - 4.0μ. See Figure 3.

The family of pyranometers receive solar radiation from the whole hemisphere. Other related remote sensing instruments, such as pyrheliometers, measure the direct solar radiation at normal incidence; pyrgeometers measure the whole hemisphere infrared radiation; pyrradiometers measure both solar and infrared radiation from a single hemisphere; and net radiometers determine the radiation balance between upward and downward directions. All these large-bandwidth instruments are helpful in determining overall local atmospheric turbidity conditions over long time periods.

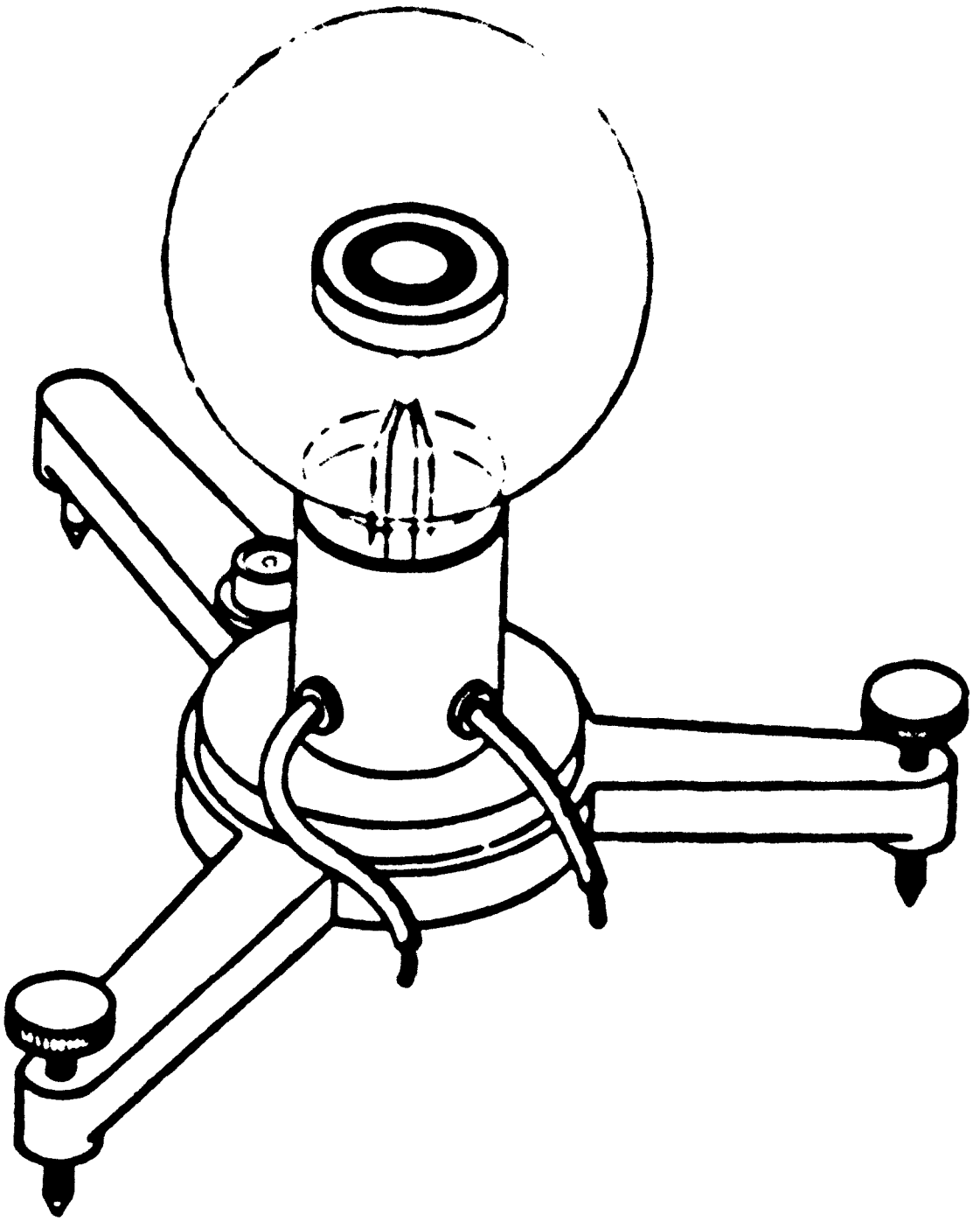

Figure 3. An Eppley pyranometer. This instrument, the basic type of which is in widespread use throughout the world, measures the total 2π ster radiation reaching a point on the earth's surface.

Using the same physical principle as described above, radiometric instruments have been placed on board space platforms to determine the global distribution of the reflected solar and long wavelength radiation leaving the earth. The reflected solar radiation and the earth's emissive long wavelength radiation occupy two separate spectral regions with little overlap. Approximately 98% of the reflected solar radiation lies in the wavelength region below 3 microns, whereas approximately 94% of the radiation emitted by the earth into space lies above 3 microns.

The sensor array shown in the photograph (Figure 4) was developed by the University of Wisconsin as adapted for flight on the TIROS Operational Satellite (TOS). The two-sensor configuration consists of a flat plate radiometer with unrestricted field of view and a flat plate radiometer set within a cone to restrict its field of view and to eliminate sensor response to direct solar radiation. This array is mounted perpendicular to the spacecraft spin axis so that the sensors scan the earth once per satellite revolution. Radiation measurements of this nature are critical to the determination of the energy balance of the earth-atmosphere system (Sellers, 1969).

The sun photometer is an optical instrument for remote sensing of atmospheric turbidity that has come into widespread use during the 1960's. This small, simple photometer was first developed by F. E. Volz (Volz, 1959). See Figure 5. It is used by the observer to make a rapid determination of the haze attenuation by measuring the direct solar radiation at a wavelength of 0.5 micron with a bandwidth of about 0.06 micron. The instrument consists of a small wooden box which contains diaphragms, filter, a bubble level, a selenium photocell sensing element whose current is measured with an enclosed microammeter, and a movable diopter mounted on a pivot outside the box. When the pivoted diopter is moved against the stop, being aligned parallel to the top of the box, it is used to aim the photometer directly at the sun. But with the instrument level and the diopter directed at the sun as before, one can read the air mass M from the scale on the inner side of the diopter.

In the determination of the haze attenuation coefficient from the measurements, the attenuation due to atmospheric molecules and the weak absorption of ozone is taken into account. Water vapor does not absorb in the 0.5 micron region. However, in more recent sophisticated versions of the sun photometer, various combinations of filters and detectors which extend the measurements into the infrared are used.

The intensity of direct solar radiation at a point on the earth's surface may be expressed in the form

$$I = \frac{I_0}{F} \; 10^{-(a_L^0 \, K\frac{p}{p_0} + B)/M} \; . \tag{3}$$

Consider the expression

$$\Delta \log I = \log I_0 - \log I - \log F \; . \tag{4}$$

By substituting expression (4) into (3), we have

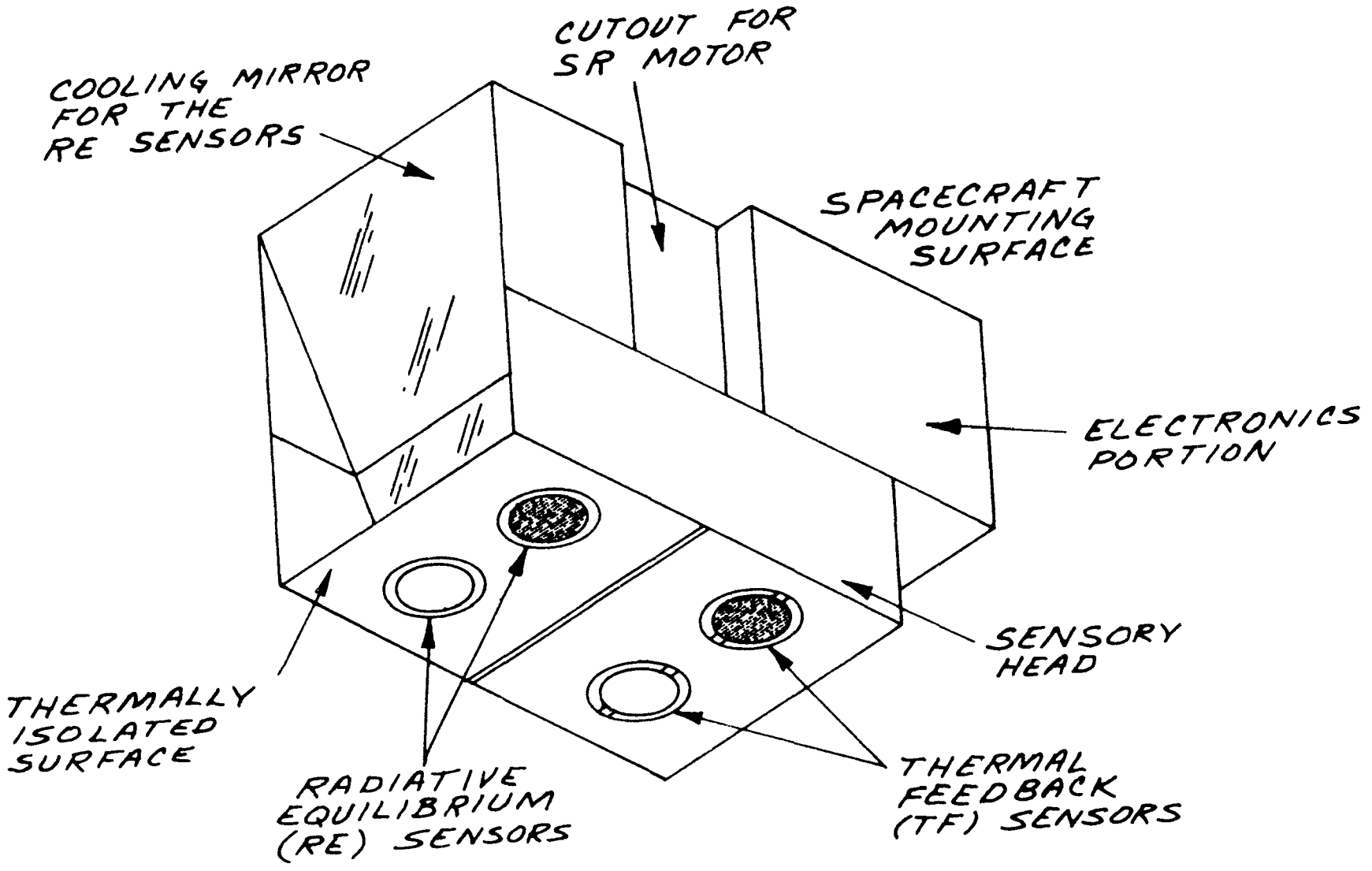

Figure 4. Flat plate radiometer.

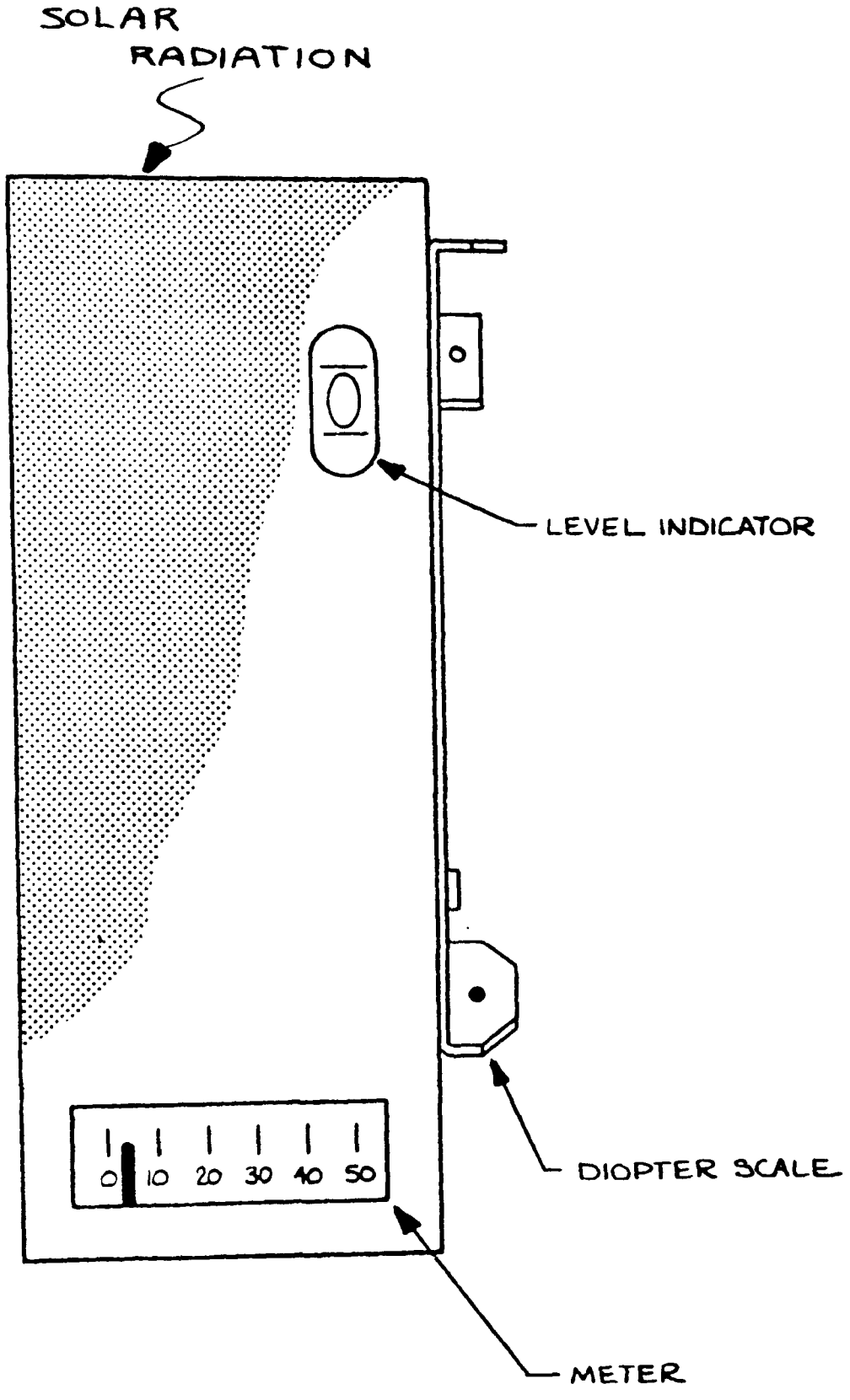

Figure 5. A schematic of a typical sun photometer.

$$\Delta \log I - a_L^0 K \frac{p}{p_0} M = BM \qquad (5)$$

where

I = the measured value of the solar radiation

I_0 = extraterrestrial value of the solar radiation. It is obtained by instrument calibration.

B = haze attenuation coefficient per unit optical path length at the particular wavelength that is being detected

a_L^0 = attenuation coefficient of pure air at the wavelength being sensed per unit optical path length at sea level

M = optical path length

K = factor to allow for the differences

p, p_0 = ambient and sea level pressure, respectively.

This section has described a few of the simple instruments that have proved extremely useful in remote sensing the atmosphere. These instruments are currently in use at many observations throughout the world.

3. Satellite Detection of Regional Pollution

We have discussed above some of the early systems whereby man began to record the contents of the atmosphere by remote-sensing techniques. Almost all early attempts made use of radiation that was transmitted and scattered by the sun. Other more modern methods not only use the sun as a source, but also starlight, reflected light from the moon, and even the natural infrared emissions directly from the aerosol constituents of the atmosphere. The above methods may be classified as passive systems, in that the source of radiation is from natural phenomena. However, remote sensing detecting systems employing their own source of radiation, such as laser radar techniques, are generally referred to as active systems.

To date all remote sensing systems on board satellites are passive. Active systems for satellites have been designed, but they have yet to be proven operational in a satellite environment. In any case, the most intriguing feature of satellite remote sensing of particulates is that by the proper data analysis one can choose local areas and short periods or large areas and long periods for investigating the properties of atmospheric pollution, and one may in this way get a handle on man-made and natural variations of turbid atmospheres. By the proper use of mathematical modeling one may then be able to estimate the strength of the source, the dispersive aspects of the pollution, and thus be in a position to forecast, at least in a crude way, global, synoptic and even mesoscale pollution variations.

It is by the use of instruments that are able to detect various broad bands of polarization radiation from the near ultraviolet (.30μ) through the near infrared (1.5μ) that one can then obtain an estimation of the particle size distribution of the turbid atmosphere. Most aerosols and particulate pollutants are readily transported and dispersed by winds. Rain-out will often remove the larger particles (> 1μ) from the troposphere, but the smaller particles ($\leq$ 1μ) essentially become long-term residents of the atmosphere, although they may agglomerate into large particles. Given suitable conditions, many of the primary pollutants (gases and particulate matter ejected directly into the atmosphere by man-made or natural means) can participate in chemical, photochemical, and/or nonchemical reactions in the atmosphere to produce secondary pollutants. The result is that the particle size distribution, and thereby the radiative spectral absorption and reflection properties will not be constant but will be extremely variable, as in the pollutant concentration, from one urban area to another, from one land mass to another—indeed, from one ocean to another and even between hemispheres. Hence, one might like to see a feasibility *integrated* program to develop the pilot instrumentation for satellite remote sensing, the mathematical computer modeling, and the procedures necessary to combine the observational and theoretical results into a system of data analysis for the purpose of forecasting pollution levels on global and synoptic scales.

A number of models describing various standard atmospheres have been proposed in order to aid in the determination of those atmospheric conditions which vary from the standard or background atmosphere. Elterman (1964) recognized that a clear standard atmosphere is a helpful concept for the interpretation of the optical properties of the atmosphere, and it can be conveniently utilized if the parameters are an array of attenuation coefficients and optical thickness values varying with altitude for each wavelength band of interest. Such a model would comprise a molecular atmosphere with a standard aerosol component. The model concept is readily workable for a molecular atmosphere and, in fact, has been computed by Deirmendjian (1955). Sekera (1956) has computed a family of curves showing the variation of the optical thickness of the molecular atmosphere with height and with wavelength. Extending this concept to include a standard particulate component is much more difficult, primarily because it varies enormously with the meteorological conditions over the polluting source.

Flower, McCormick and Kurfis (1969) analyzed five years of turbidity measurements made with a Volz sunphotometer from a network of stations in the United States. They found among other things the mean turbidity to be higher in the eastern regions than in the western regions, and an annual cycle of low winter turbidity and high summer turbidity. McCormick and Ludwig (1967), from other ground-based data, showed a large worldwide increase in turbidity over the last 50 years. Hanson (1969), in studying the use of Rayleigh scattering viewed by a geostationary satellite as a measure of various atmospheric parameters, concluded that for small values of satellite-sun angles and for relatively large wavelengths ($\lambda \equiv .7\mu$), the radiance for aerosols appears to be about three times greater than from molecular scattering.

As far as remote sensing from above is concerned, the problem is complicated by the variation in albedo of the surface from which the pollution originates and over which it moves. Another difficulty which besets this method of aerosol pollution surveillance, is the non-Lambertionality of the reflecting earth's surface. These are the two most important problems which have to be solved before one can begin an attack on the development of a method of detecting the variation of particulates on a local and on a global scale by satellite remote sensing.

Sellers (1969), in modeling the global climate, based his work on the concept that the steady-state average latitudinal distribution of surface temperature, to a first approximation, should depend greatly on the incoming solar energy, the transparency of the atmosphere, and the planetary albedo. From Figure 5 of Sellers' paper we see strong dependency of the mean annual temperatures on various assumed polar albedos.

There is little doubt that the constituents of the atmosphere have an enormous impact on the climate of the earth. Water vapor, carbon dioxide and other major components of the atmosphere have the greatest impact on global climatological parameters, whereas particulate matter such as dust and aerosols, which is indeed a major component of the atmosphere, has an impact on climate both on a global scale as well as regional. The magnitude and cause of this impact is being debated in the scientific literature (Bryson, Mitchell, Rasool and Schneider).

Whether or not global long-term climatic changes are due to the increasing man-made particulate loading of the atmosphere or due to natural particulate loading from volcanic eruptions, it is certain that regional changes in particulate loading do indeed affect the temperature, rainfall and radiation reaching the earth's surface (Barrett et al., 1970).

This phenomenon is borne out in a number of special situations. The strong decrease of atmospheric optical radiation observed in the northern hemisphere after volcanic eruptions of Krakatoa, 1883, and Katmai, 1912 (Volz, 1965), as well as the more recent explosion of the Agung volcano, 1963 (Volz, 1970) located at Bali Island in the southern hemisphere, injected dust into the atmosphere that spread over the entire hemisphere and remained airborne for a number of months.

Mohr (1971) correlated two ESSA 8 satellite pictures of western and central Europe to show that a satellite could locate an existing low-level inversion over a large regional area in a situation that is cloud free and that a certain minimal amount of pollution is present. In Figure 6 the atmosphere is relatively clear (marked "+"), whereas in Figure 7 the atmosphere over the same area (marked "C") at a later date is polluted. Both pictures were received by automatic picture transmission (APT) by Deutscher Wetterdienst, Offenbach/Main, Germany. Figure 6 shows a large clear area over northcentral and western Europe on 18 June 1970. The coastlines along the Baltic and North Seas are sharp and distinct, and most of England is visible. Central Europe and southern Scandinavia are under the influence of the southeastern edge of an anticyclone centered in the Norwegian Sea. A very dry northeasterly airflow dominated the area (marked "+"). The range of dry-bulb/wet-bulb temperature separations was

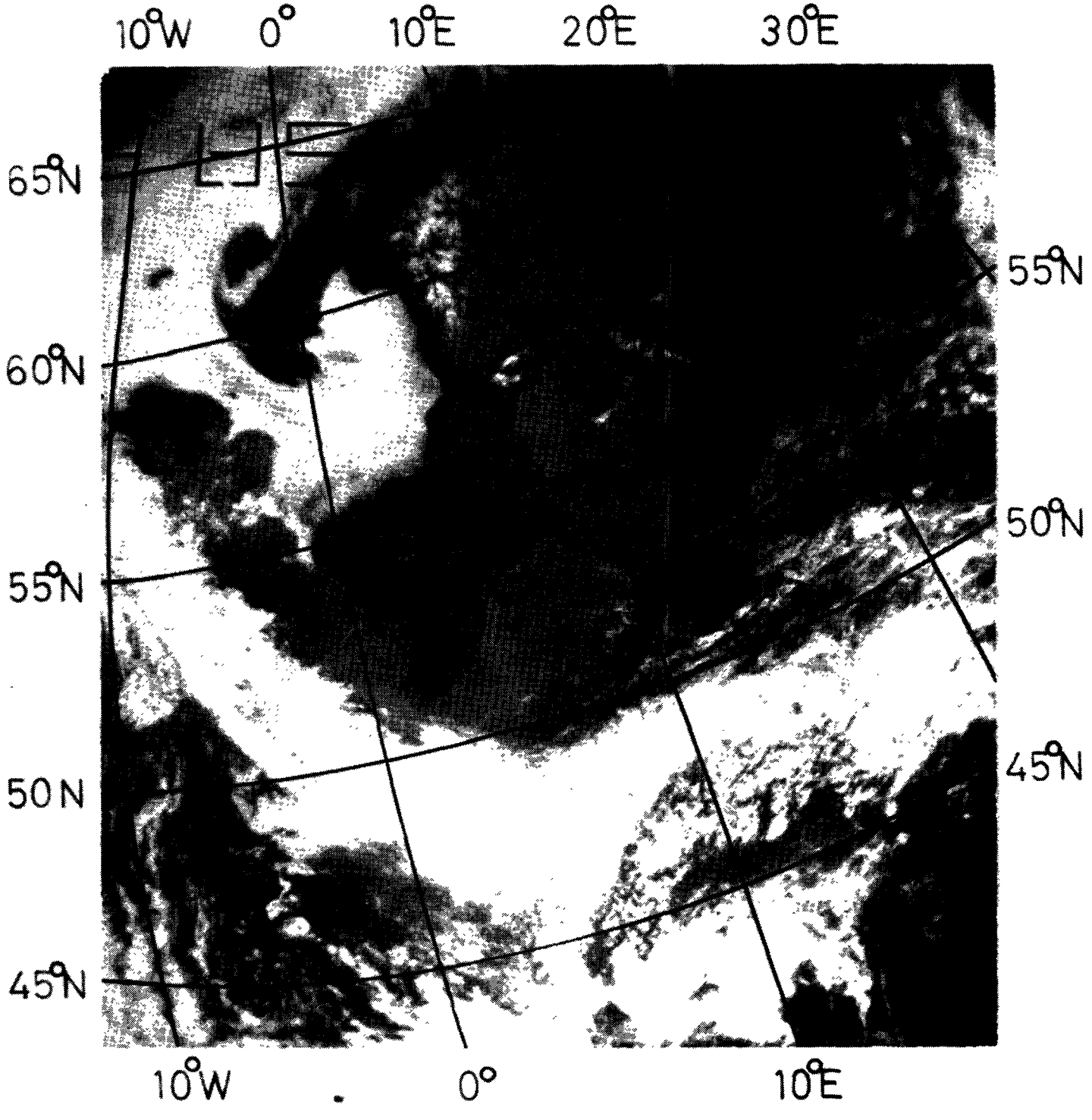

Figure 6. ESSA 8 photograph at 1001 GMT on 18 June 1970. Note the clear skies over northcentral and western Europe.

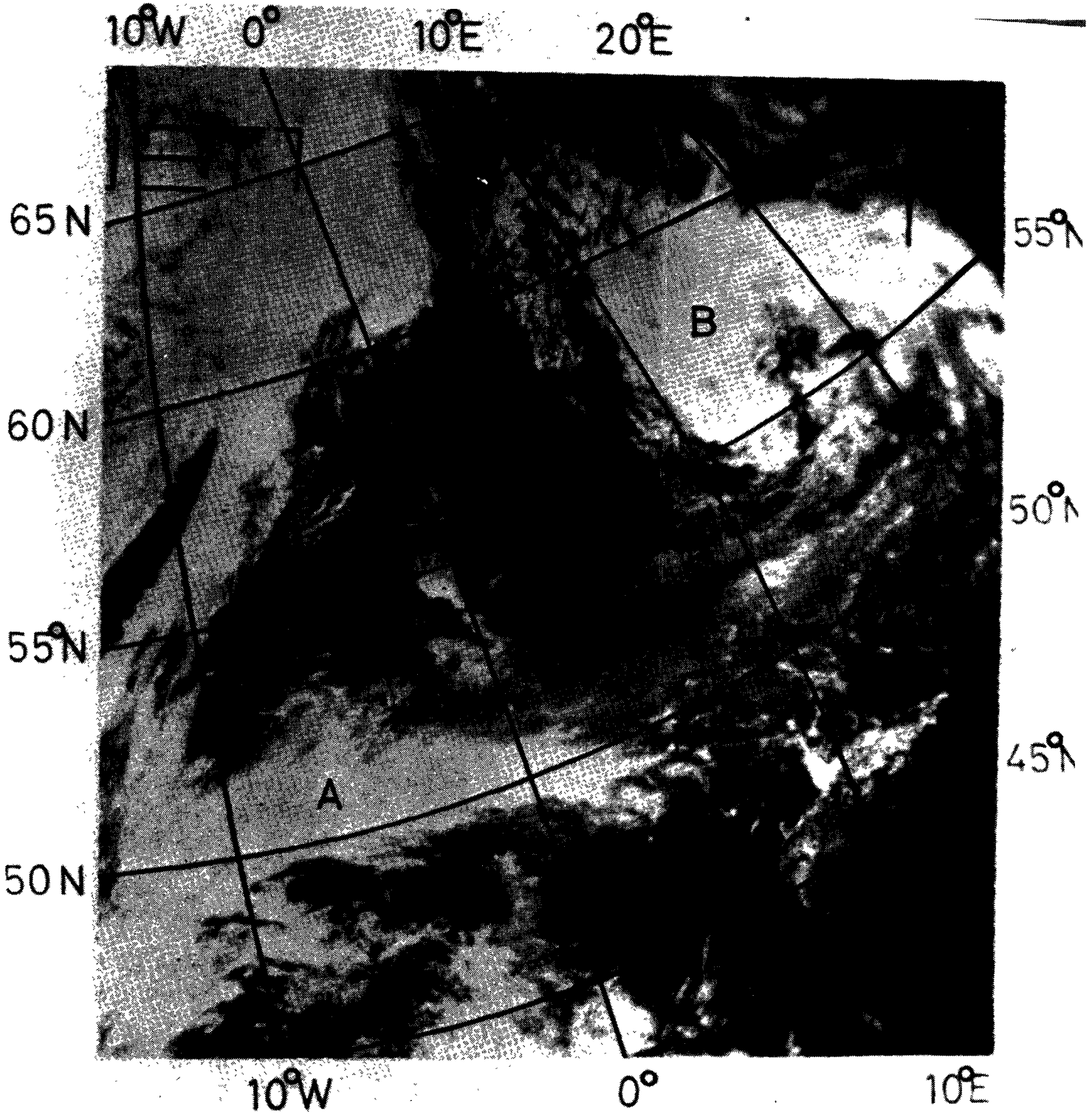

Figure 7. ESSA 8 photograph at 1046 GMT on 5 August 1970. Note the extensive area of atmospheric pollution located at C.

Figure 8. A geographical map of the central Europe region.

between 15° and 20°C. Visibilities in northern Germany were reported in the 25- to 40-kilometer range, and maximum temperature reached 25°C. Note the fog forming in the easterly flow over the northern part of the North Sea and the clear area in the lee of northern Scotland and the Shetlands.

However, the situation on 5 August 1970 was quite different. (See Figure 7.) A ridge of relatively high pressure lying between a low over the Bay of Biscay and a weak low over the Baltic Sea (B) dominated central Europe. The coastlines that showed so clearly in Figure 6 are now obscured in Figure 7 by haze in the moist maritime air that was moving onshore. The band C extending from the frontal zone at A has the appearance of dense cirriform cloudiness. Figure 8 is a geographical map of the area. Although only a few stations in this area reported cirrus, all stations recorded dust or haze. Temperatures reached a maximum of about 27°C, relative humidity values were between 70% and 80%, and visibilities ranged beteen 1.5 to 6 kilometers. Therefore, one may assume that the band C represents a large regional area of air pollution with haze and dust trapped below the temperature inversion. This band lies over a heavily industrialized region where the effluents emitted by factories and the unfavorable atmospheric conditions of the low-level inversion and light surface winds combined to produce this regional pollution situation. This situation is not unlike that which often occurs over the northeastern part of the United States.

4. Satellite Detection of the Movement of Large-scale Man-made Pollution

An example of large-scale man-made particulate loading is exemplified by agricultural slash burning operations carried out throughout the world in certain seasons. The most striking operations occur annually in Africa and in South and Central America. In Guatemala, the annual slash burning operations usually begin in February and last until the onset of the rainy season in May. Parmenter (1971) has pointed out that the airborne pollution from this large-scale burning operation in Central America can be viewed from satellite, and he showed that the smoke pattern can be followed in space and time by means of Applications Technology Satellite III (ATS-III) spin-scan camera system. Figure 9 shows a series of ATS-III pictures that show the smoke for a 25-day period from 18 April 1971 to 12 May 1971. From these photographs, the smoke appears to originate in two areas: Tabasco, Mexico and the lowlands along the Gulf of Honduras. This entire area was located in the southwest quadrant of a high for the first 12 days of ATS coverage. The resulting southerly flow carried the smoke from the land northward across the Gulf of Mexico as far north as New Orleans, Louisiana. The smoke was only slightly visible in the first picture as outlined by the dotted line. On the next day, 19 April, the smoke from the two sources extended offshore and was more dense. On 22 and 23 April, the smoke covered a large area of the lowlands north of the Sierra Madre range and extended northward to the front located near the southern coastline of the United States. To the end of April, the anticyclonic flow continued to carry smoke northward and eastward in advance of the front to the point that it covered the western half of the Gulf of Mexico.

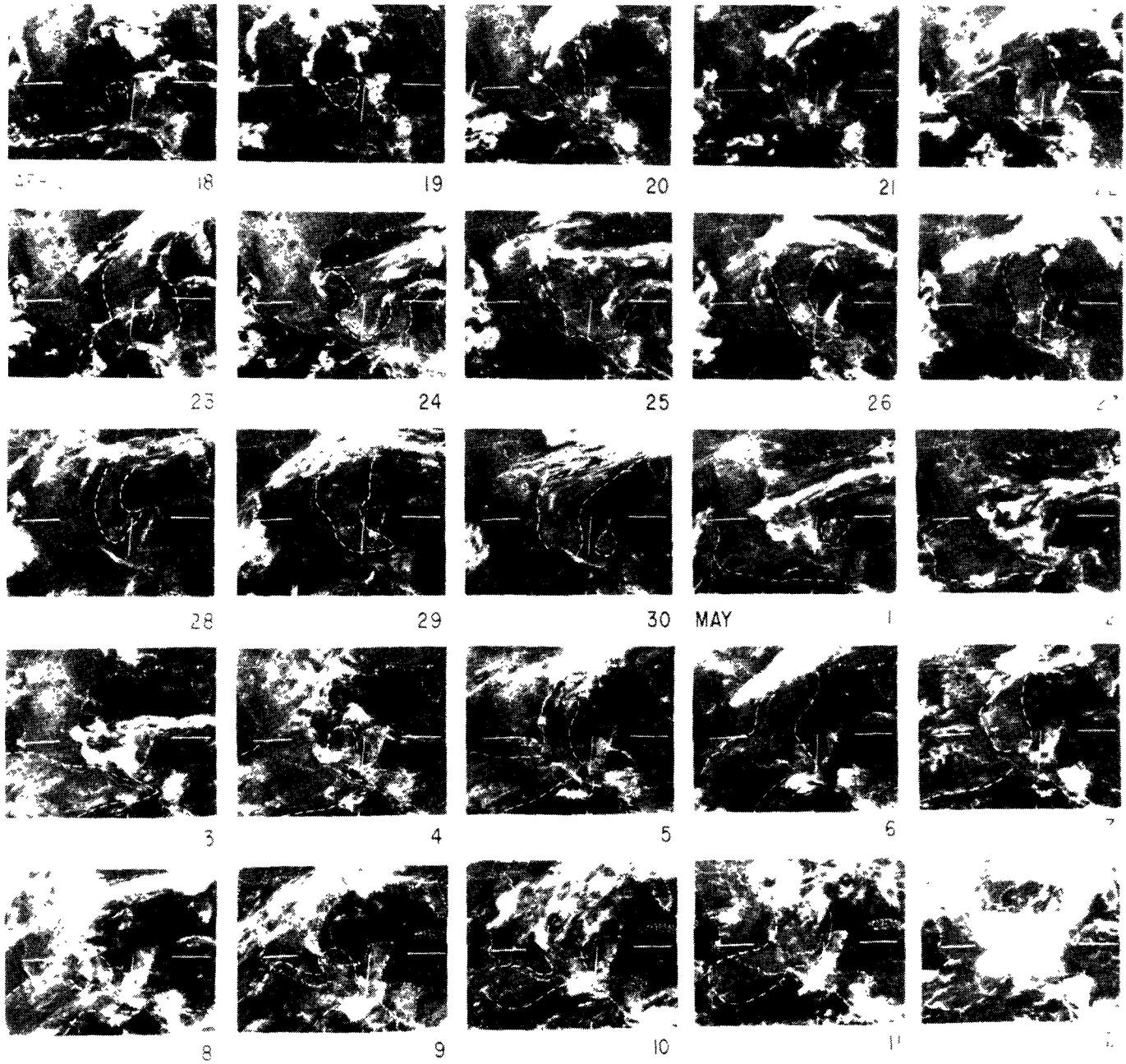

Figure 9. A series of ATS-III pictures showing the tracking of large-scale man-made pollution. Smoke from agricultural slash burning operations in Central America from 18 April to 12 May 1971.

On 1 May a strong frontal system moved into the Gulf with a change in fog and stratus clouds, with the result that the smoke moved southward across southern Mexico and out over the Pacific Ocean. A subsequent change in low-level flow which occurred on 4 May once again caused the smoke to drift northward across the Gulf of Mexico while it gradually diminished over the Pacific. A large covering frontal system brought moderate rain to the region on 12 May, thereby ending the burning season in Central America. Even at this time in which the source was being cut off, smoke could still be seen over the Pacific. This is an interesting example showing the feasibility of satellite tracking of pollution originating from what is essentially a point source, then moving over thousands of kilometers.

5. Urban Modeling for Air Pollution Detection

In detecting pollution between a detector and a surface by means of remote sensing, it is often necessary to consider in some detail the physical structure of the surface. This is especially true if one is concerned with polarization studies, but it is also true for a remote sensing study involving any wavelength of light, even into the infrared where the surface itself is the emitter. In the investigation of the intervening atmosphere between a surface and observer, we must first be concerned with the light intensity emerging from a portion of a surface S. The surface may not be a real surface, such as a case where one has a dense hazy atmosphere with an extremely large optical depth in which multiple scattering predominates, or the surface may be the actual radiating source, or an illuminated surface. For our particular case we will consider the reflected light from an opaque surface.

Let $P(x,y,z)$ be a point on the reflective surface where the coordinates (x,y,z) refer to any point on this surface. Even though we are considering a truly two-dimensional surface, we will describe it with the three Cartesian coordinates, most suitable for a city with flat planar streets and roof tops and with buildings with high vertical sides. The average amount of energy which is reflected per unit of time from an infinitesimal surface element δS at the point P and within an element $\delta\Omega$ of solid angle around a direction specified by the polar angles (α,β), can be expressed in the form

$$J = B(x,y,z;\alpha,\beta) \cos\theta \, \delta S \, \delta\Omega \, , \tag{6}$$

where θ is the angle which the vector (α,β) makes with the normal to the surface δS (see Figure 10). The term $\cos\theta$ is introduced into Eq. (6) because it is the projection of δS onto a plane normal to the direction (α,β) which is the physically significant quantity, rather than δS itself. The reflected brightness B is a very complicated function of the five coordinates $(x,y,z;\alpha,\beta)$ with the constraint

$$f(x,y,z) = 0 \tag{7}$$

which specifies the two-dimensional reflective surface. For a complete solution to the problem of remote sensing atmospheric pollution by means of reflective radiation, B must be known as a function of the above five

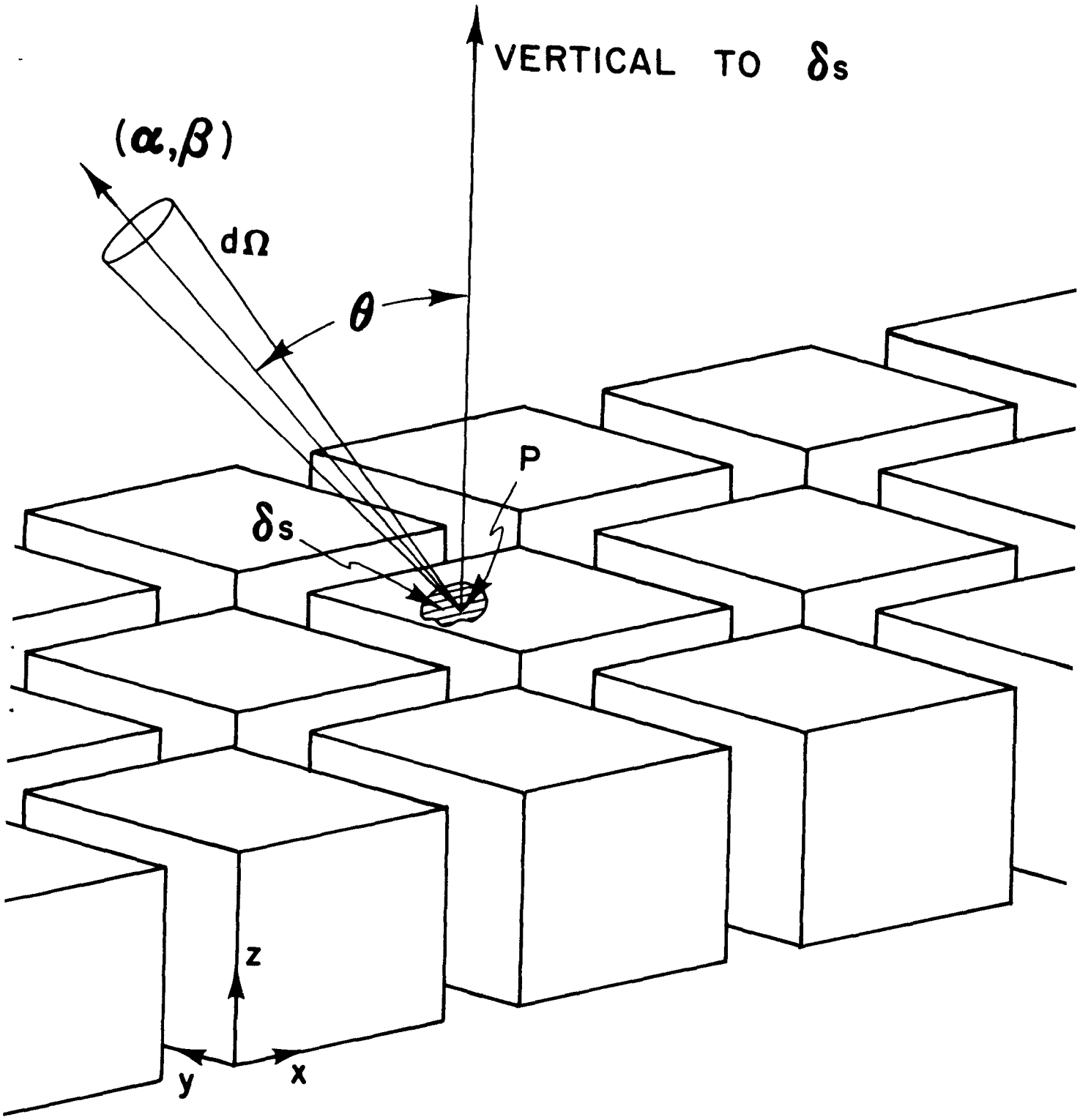

Figure 10. Geometry of model for radiation scattered from urban areas. Symbols are defined in the text.

coordinates as well as a function of wavelength. Polarization parameters may be included for completeness. However, in many practical cases when only limited results need be known, a number of approximations can be employed.

The photometric intensity is defined as

$$\delta I = \delta f/\delta\Omega = B \cos\theta \, \delta S \, . \tag{8}$$

Upon integrating, we have

$$I(\alpha,\beta) = \int B \cos\theta \, ds \, . \tag{9}$$

The brightness B at the point P depends, of course, on the nature of the surface, whether it is rough or smooth, whether it is self-radiating (infrared), or whether it is reflecting other light (multiple scattering within the atmosphere). In the analysis of remote sensing data over oceans, forests and flat desert areas, it is often permissible to assume, to a good approximation, that the radiation is isotropic, that is, that B is independent of direction. If we also assume the radiating surface to be a plane, Eq. (9) becomes

$$I = I_0 \cos\theta, \tag{10}$$

where

$$I_0 = \int B \, ds \, . \tag{11}$$

Equation (11), Lambert's cosine law, states that the photometric intensity in any direction varies as the cosine of the angle between that direction and the normal to the surface. The analysis of the Los Angeles ATS-III data assumes essentially that the reflecting surfaces of the ocean, desert and city are identical, which of course they are not.

A flight was made over the downtown areas of Madison and Milwaukee, Wisconsin, and Chicago, Illinois, in order to determine the urban ratio of total rooftop area to total street area, the urban building height to street width ratio, as well as the overall surface albedo of building sides, building tops and street-sidewalk areas. The flight was made in a 4-seat 172 Cessna Skyhawk. William Kuhlow and David Cadle photographed the urban regions with a Bronica S 2 1/4 by 2 1/4 still camera and a Bolex 16 mm Rex movie camera with various filters.

Efforts are underway at the present time to model the reflectivity of a typical city, that is, to determine B for various source angles, observing angles, and wavelengths. Construction has been completed on a model city with an appropriate building-height to street-width ratio and with appropriate street, building-side and rooftop albedos. The cardboard model city consists of 18 blocks, each of which may be viewed as a city block or an individual building, located on an area of 55 cm by 60 cm (3300 cm^2). Each block covers an area of about 8 cm by 10 cm (80 cm^2). The height of each block (building) is approximately 8 cm, and the distance between each block (street width) is 4 cm. All rooftops are flat. The total rooftop area is 1440 cm^2 and the total street area is 1860 cm^2. The

ratio of the total rooftop area to total street area is .78, the rooftop area is about 45% of the total citywide area, the street area is about 55% of the total area, and the ratio of the height of each building to the width between buildings is 2. The streets were painted a flat beige color, the sides of the buildings were painted with flat gray enamel, and their tops were painted semiflat black. The detail specifications were as follows:

1) Streets: Brand name KRYLON (Borden)
Beige enamel No. 2504
Pigment 4.90%
Telanium Dioxide 83.30%
Iron Oxide Yellow 14.10%
Iron Oxide Red 2.10%
Carbon Black .50%

Nonvolatile 8.9%
Cellulose Nitrate
Oil-Free Alcohol Derived Alkyd
Coconut Oil Alkyd
Dioctyl Phthalate

Volatile 8.9%
Ketones
Esters
Alcohols
Aromatic, Aliphatic and Halogenated Hydrocarbons

2) Sides: Brand name KRYLON (Borden)

Smoke Gray No. 1608
Federal Color Standard 595 No. 16187
Pigment 2.58%
Titanium Dioxide 94.68%
Carbon Black 2.58%
Iron Blue 1.54%
Iron Oxide Yellow 1.20%

Nonvolatile 13.03%
Cellulose Nitrate
Oil-Free Alcohol Derived Alkyd
Coconut Oil Alkyd
Dioctyl Phthalate

Volatile 84.38%
Ketones
Esters
Alcohols
Aromatic, Aliphatic and Halogenated Hydrocarbons

3) Tops: Brand Name KRYLON (Borden)

Semiflat Black No. 1613
Pigment 1.55%
Lampblack 71.5%
Silicates 28.5%

Nonvolatile 8.80%
Cellulose Nitrate
Dioctyl Phthalate
Secondary Amines

Volatile 89.65%
Ketones
Esters
Alcohols
Aromatic, Aliphatic and Halogenated Hydrocarbons

The laboratory setup for this urban scattering experiment is shown in Figure 11. The spectrophotometer is viewing the model city at an angle 30° south from the nadir. The light source, which was a Sylvania No. 2 Superflood EBV 110-120 V, was located southwest of the model city. The angle of the sun above the horizon, ψ, as seen from the model city, was set at three different positions for each experiment. These positions were 20°, 40° and 60°. Each experiment consisted of varying the filters in the spectrophotometer. Figure 12 shows the results of the visible radiation, Figure 13 the infrared, and Figure 14 the polarized visible. The data were taken in increments of 10° as the model city was rotated in the horizontal plane. For isotropic scattering off a flat horizontal plane, the results would graph as a circle, the radius of which would be proportional to the intensity. Deviations from a circle show the effect which the orientation of the streets (alignment of buildings) has upon the angular variation of the reflected radiation, with respect to the source-detector angles. As can be seen in all three graphs, the higher the source is over the horizon, the more intense the reflected radiation. Also, in the visible and infrared studies, the lower the source is to the horizon, the larger the percentage change of angular variation. However, this is not the case in the polarization studies. In the situation of observing the reflected visible polarized radiation, there is a strong dependency on street orientation with respect to the source-detector angle with an increase in source altitude. This point emphasizes the care which must be taken in interpreting polarization studies of non-Lambertian reflectors.

6. Summary and Recommendations

We have outlined in this paper the early methods and instruments that man used for remote sensing the state of the atmosphere. The most recent development, that of satellite observations, differs markedly from all earlier methods, since the remote sensing observations are made from above the atmosphere. The scope and range of satellite observations in detecting atmospheric pollution were shown to vary from urban areas to the global scale. A modeling experiment was carried out to determine the

variation in radiation reflected from a city through an optically thin atmosphere.

From this work we have seen that there is a profound difference between viewing atmospheric pollution with older instruments from the ground and with satellites from above. It was not that the difference was in the more modern sophisticated instruments. Indeed, some of the early satellite radiometers, even though they were quite primitive in operation, yielded startling results. Rather, the satellite observations required a knowledge of the optical properties of the earth's surface below the pollution for proper interpretation of their results. In the study of cloud motions by analysis of satellite data, the earth surface areas are used only for navigation, and this could be done because the optical depth through most clouds is small. (However, this is not true for high cirrus shields.)

Thus for further study of atmospheric pollution from satellite data, we recommend that an investigation of the optical properties of various earth surfaces be undertaken. When the properties of reflected light through a clean atmosphere from a particular surface are known, it will be possible then to say something about a) observed deviations from this norm and b) the particulate loading of the intervening atmosphere.

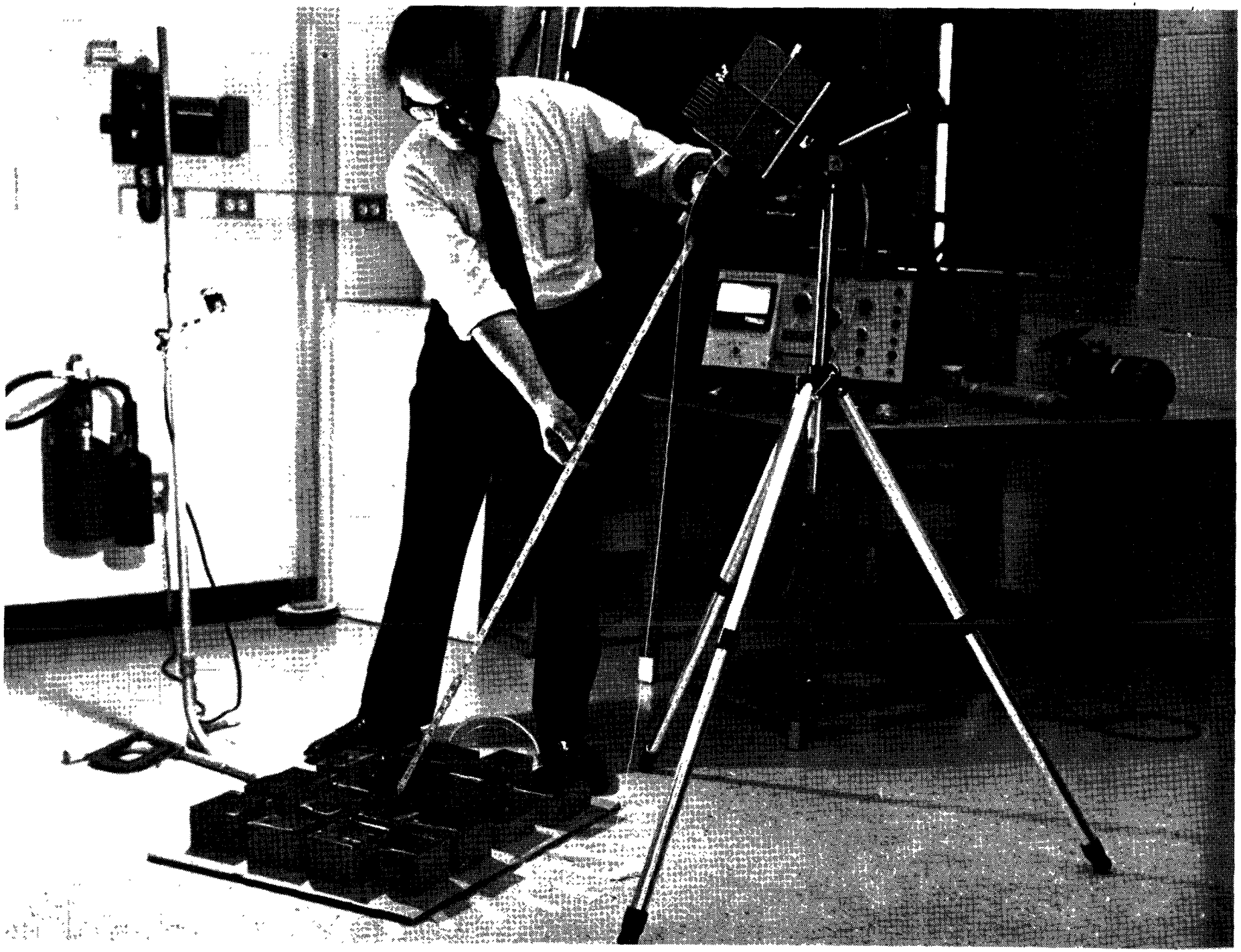

Figure 11. Laboratory setup for the urban scattering experiment.

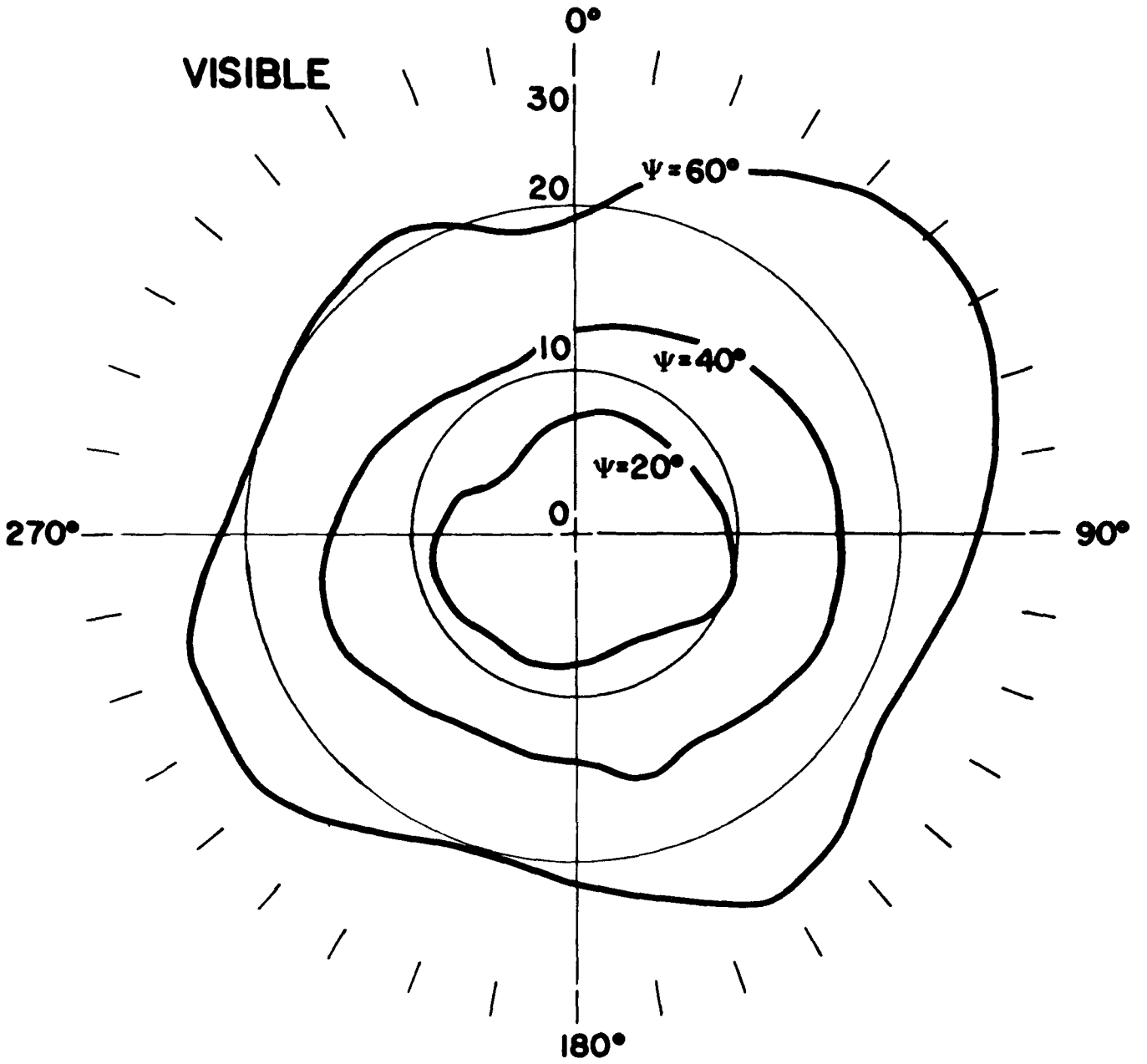

Figure 12. Reflection amplitude of visible radiation for 0-360° street angles for three source positions.

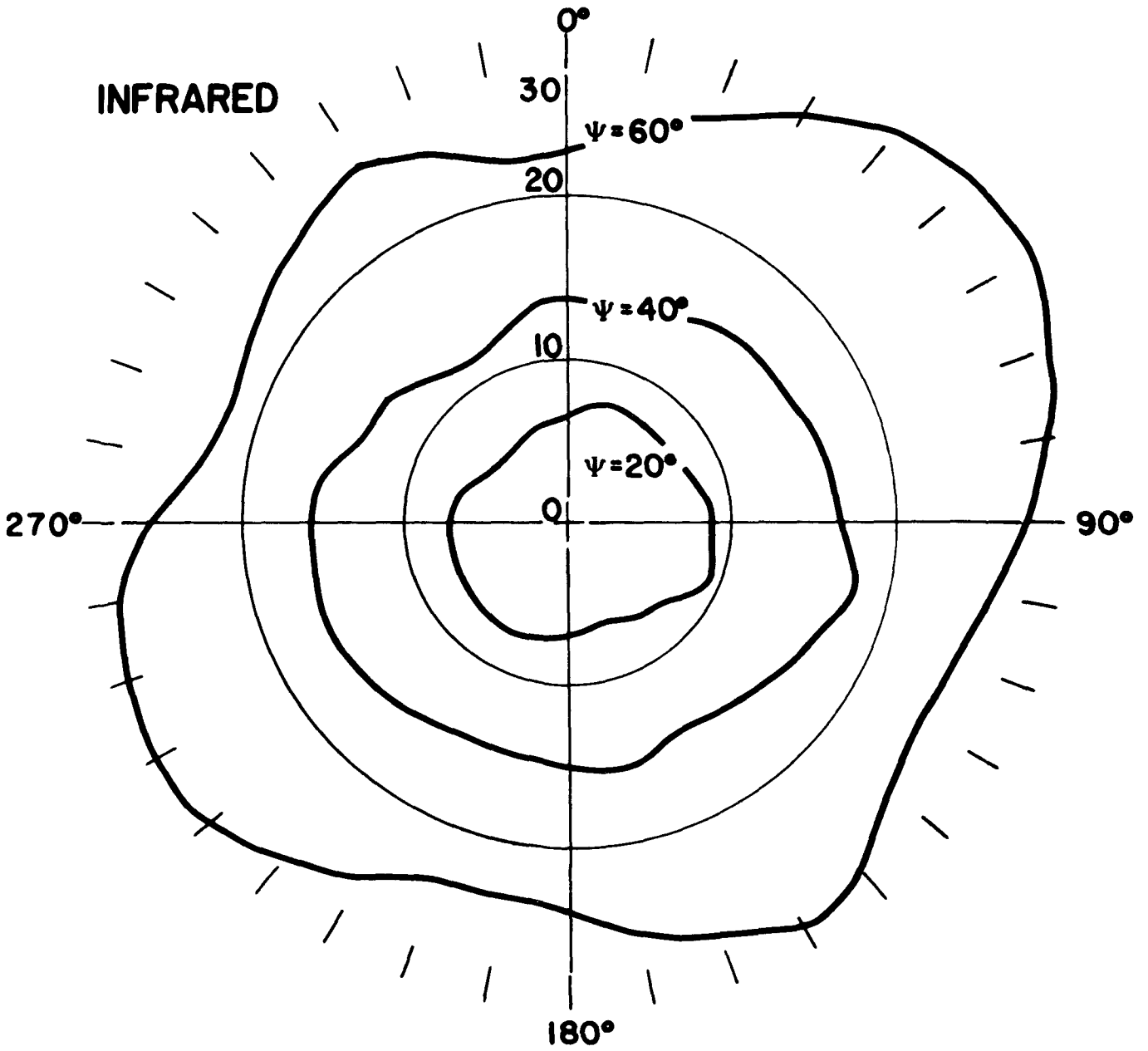

Figure 13. Reflection amplitude of infrared radiation for 0-360° street angles for three source positions.

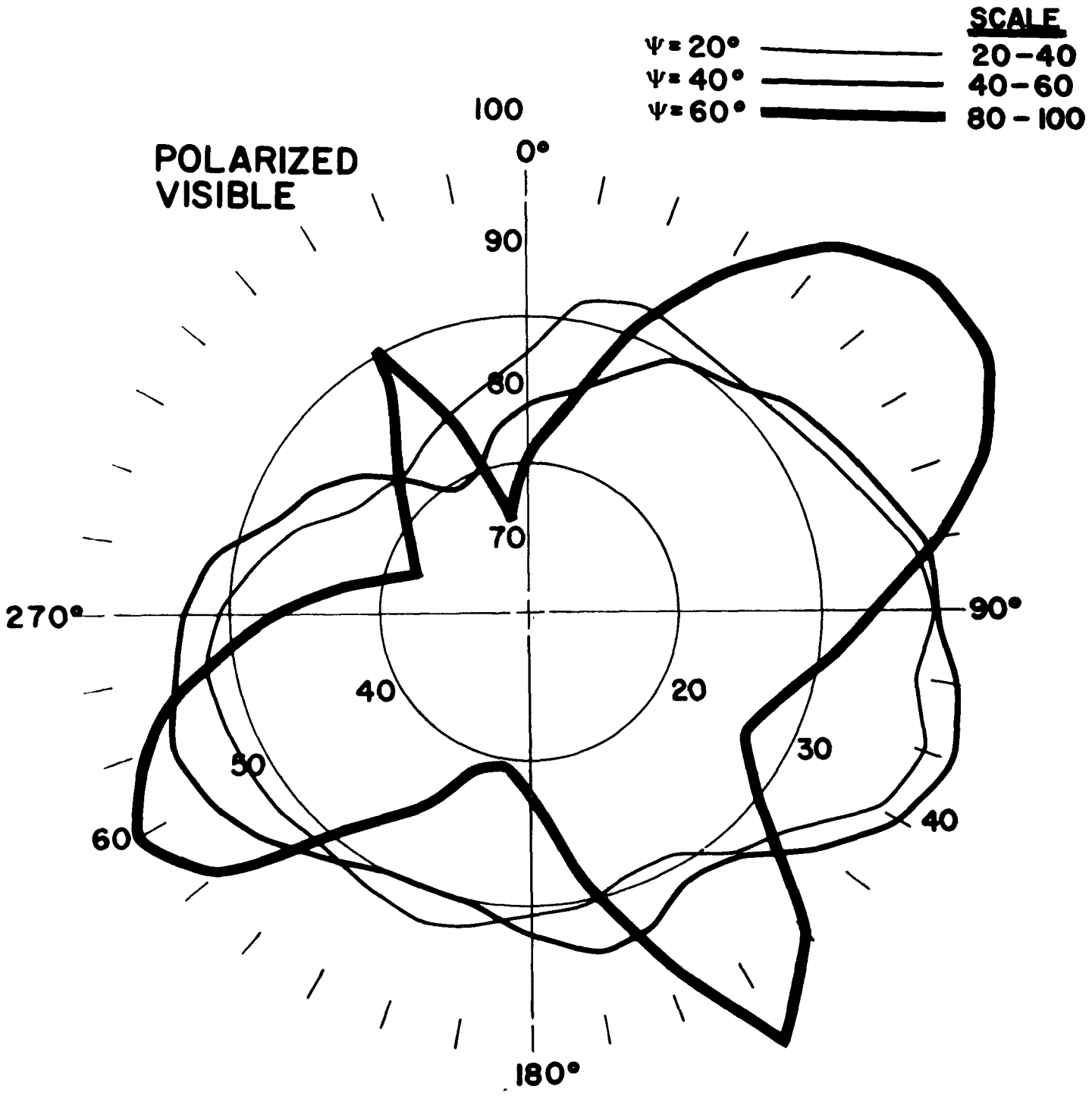

Figure 14. Reflection amplitude of polarized visible radiation for 0-360° street angles for three (unpolarized) source positions.

References

Atwater, N. A., 1970: "Planetary Albedo Changes Due to Aerosols," *Science* 170, 64-66.

Barrett, E. W., R. F. Pueschel, H. K. Weickmann, and P. M. Kuhn, 1970: "Inadvertent Modification of Weather and Climate by Atmospheric Pollutants," ESSA Technical Report ERL 185-APCL 15, Boulder, Colorado, 103 pp.

Bricker, O. P. and J. M. Prospero, 1969: "Airborne Dust on the Bermuda Islands and Barbados," *EOS Transactions* 50, 176.

Bryson, R., 1971: "Climatic Modification by Air Pollution," Paper presented at International Conference on Environmental Future, Helsinki, Finland, 36 pp., 27 June - 3 July 1971.

Bryson, R. A., and W. M. Wendland, 1970: "Climatic Effects of Atmospheric Pollution," in *Global Effects of Environmental Pollution*, ed. S. F. Singer (New York: Springer-Verlag), pp. 130-138.

Burns, F. A., 1961: "Dust Haze in Relation to Pressure Gradients," *Meteorological Magazine* 90, 223-226.

Cox, S. K., K. J. Hanson, and V. E. Suomi, "Measurements of Absorbed Shortwave Energy in a Tropical Atmosphere," Paper presented at the Conference of the International Solar Energy Society.

Deirmendjian, D., 1969: *Electromagnetic Scattering on Spherical Polydispersions*, Elsevier Publishing Company.

Deirmendjian, D., 1955: *Arch. Meteor. Geophys. Bioklimator. Ser.* B6, 452.

Elterman, L., 1964: "Parameters for Attenuation in the Atmospheric Windows for Fifteen Wavelengths," *Applied Optics* 3, 745.

Fischer, W. H., 1967: *J. Appl. Meteorology* 6, 958.

Fischer, W. H., 1971: *Science* 171, 828.

Flowers, E. C., R. A. McCormick, and K. R. Kurfir, 1969: "Atmospheric turbidity over the United States," *J. Appl. Met.* 8, 955.

Hanson, K. J., 1969: "Applications for Bispectral Radiance Measurements from a Satellite,: Ph.D. Thesis, Department of Meteorology, University of Wisconsin, Madison.

Kondrat'yev, K. Ya, 1965: "Actinometry," National Aeronautics and Space Administration, NASA TT F-9712, 675.

Lettau, H. and K. Lettau, 1969: "Shortwave Radiation Climatonomy," *Tellus* 21, 208.

Lodge, J. P. and J. B. Pate, 1966: "Atmospheric Gases and Particulates in Panama," *Science* 153, 408.

McCormick, R. A. and C. Ludwig, 1967: "Climatic Modification by Atmospheric Aerosols," *Science* 156, 1358.

Middleton, J. T., 1971: "Planning Against Air Pollution," *American Scientist* 59, 188.

Middleton, W. E. K., 1969: *Invention of Meteorological Instruments*, Johns Hopkins Press, Baltimore, Maryland.

Mitchell, J. M., 1961: "Recent Secular Changes of Global Temperature," *Annals of the New York Acad. Sci.* 95, 235.

Mitchell, J. M., 1970: "A Preliminary Evaluation of Atmospheric Pollution as a Cause of the Global Temperature Fluctuation of the Past Century," in *Global Effects of Environmental Pollution*, ed. S. F. Singer, Springer-Verlag, New York, pp. 137-155.

Mohr, T., 1971: "Air Pollution Photographed by Satellite," *Monthly Weather Review* 99, 653.

Morgan, G. B., G. Ozolins, and E. C. Tabor, 1970: "Air Pollution Surveillance Systems," *Science* 170, 289.

Porch, W. M., R. J. Charlson, and L. F. Radke, 1970: "Atmospheric Aerosol: Does a Background Level Exist?" *Science* 170, 315.

Prospero, J. M., 1968: Atmospheric Dust Studies on Barbados," *Bull. of the American Meteorological Society* 49, 645.

Prospero, J. M., and T. N. Carlson, 1970: "Radon-222 in the North Atlantic Trade Winds: Its Relationship to Dust Transport from Africa," *Science* 167, 974.

Prospero, J. M. and T. N. Carlson, 1971: "Radon-222 and African Dust in the North Atlantic Trade Winds," Bomex Bulletin #10, NOAA, 2-10, June 1971.

Prospero, J. M., E. Bonatti, C. Schubert, and T. N. Carlson, 1970: Dust in the Caribbean Atmosphere Traced to an African Dust Storm," *Earth and Planetary Science Letters* 9, 287.

Rasool, S. I. and S. H. Schneider, 1971: "Atmospheric Carbon Dioxide and Aerosols: Effects of Large Increases on Global Climate," *Science* 173, 138.

Scorer, R. S., 1969: *Air Pollution*, Pergamon Press, London.

Sekera, Z., 1956: *Advances in Geophysics* 3, 43.

Sellers, W. D., 1969: "A Global Climatic Model Based on the Energy Balance of the Earth-atmosphere System," *J. Applied Meteorology* 8, 392.

Tepper, M. and S. Ruttenberg, 1970: "The Role of the Satellite in Future Observing Systems," *Meteorological Monographs* 11, 56.

Volz, F. E., 1959: "Photometer mit Selen-Photoelement zur spektralen Messung der Sonnenstrahlung und zur Bestimmung der Wellenlaengenabhaengigkeit der Dunsttruebung," *Archiv. für Meteor., Geophys., Bioklim.* B10, 100.

Volz, E. E., 1965: "Note on the Global Variation of Stratospheric Turbidity Since the Eruption of Agung Volcano," *Tellus* 17, 513.

Volz, F. E., 1970: "Spectral Skylight and Solar Radiance Measurements in the Caribbean: Maritime Aerosols and Sahara Dust," *J. Atmos. Sci.* 27, 1041.

Volz, F. E., 1970: "On Dust in the Tropical and Midlatitude Stratosphere from Recent Twilight Measurements," *J. of Geophys. Res.* 75, 1641.

Volz, F. E., 1970: "Atmospheric Turbidity after the Agung Eruption of 1963 and Size Distribution of the Volcanic Aerosol," *J. of Geophys. Res.* 75, 5185.

Wolkonsky, P. M., *Arch. Environ. Health* 19, 586.

IV — RAYLEIGH-GANS-BORN LIGHT SCATTERING BY ENSEMBLES OF RANDOMLY ORIENTED ANISOTROPIC PARTICLES*

ABSTRACT:

A formula for the electromagnetic scattering amplitude is presented. Using the Rayleigh-Gans-Born approximation, we apply it to the calculation of Stokes matrices for ensembles of randomly oriented anisotropic particles. Two types of anisotropy are treated in detail: particles of any shape with a variable scalar refractive index $n(\vec{r})\delta_{ij}$ and spherical particles with a constant tensor refractive index n_{ij}. For a monodisperse ensemble of the second type, we describe a method of extracting from data a shape parameter γ. One may be able to generalize this method to yield structural information for a wider class of ensembles.

*Paper accepted for publication in *Applied Optics*.

1. Introduction

Ever since the original investigations by Tyndall (1869) [1] and Rayleigh (1871) [2] of the effects of small particles upon incident light, scattering of electromagnetic radiation has been a potent tool for scientists. Chemists and biologists have used the scattered radiation to study the structures of colloidal suspensions, macromolecules and polymers [3]— astronomers to study interstellar dust and to deduce from polarization interstellar magnetic fields [4].

The effects of aerosols on man and, conversely, the effects of his activities on the aerosol content of the atmosphere are now undergoing intensive scrutiny by environmental scientists. The influence of aerosols upon global climate is one of the most debated issues in atmospheric science [5]. Will the aerosols produced by volcanic activity, and by man's slash-and-burn agricultural, industrial and automotive activities, tend to increase or decrease the mean surface temperature of the earth? Which have the greater influence upon climate— volcanic or man-made aerosols? To answer these questions, one must understand the light scattering and absorbing properties of different kinds of aerosols [6].

Knowledge of the optical signature of each aerosol may enhance legislative control of air quality, since one may be able to identify violators by tracing an aerosol to its point of origin by remote sensing from satellites or from a network of monitoring stations.

Finally, just as studies of the optical properties of interstellar dust have provided information about interstellar magnetic fields, so also a deeper understanding of the optical properties of the earth's aerosols (i.e., atmospheric dust) might lead to further knowledge about the motions of the earth's atmosphere and about its electromagnetic fields.

In solving radiative transfer problems, most atmospheric physicists treat an aerosol as if it were an ensemble of homogeneous spheres differing in size and refractive index [7]. Their motivation in choosing such a model is that it is the only one for which an exact solution exists for the scattering amplitude (Mie, 1908)[8], even when the size of the particle is approximately equal to the wavelength of the radiation.

This model's flaw is that details of the structure of the particles forming the aerosol are omitted. Thus, one cannot describe correctly the polarization of the scattered light [9]. Holland and Gagne have shown that Mie theory is not only unable to fit the polarization data of a known aerosol, but also is unable to fit the backscattered intensity [10]. Understanding backscattering is crucial for the interpretation of aerosol data accumulated by satellites [11]. We, therefore, are interested in studying the effects of anisotropic particles upon an incident beam of electromagnetic radiation.

A suitable method for describing the optically measurable quantities for a scattering process is to employ the Stokes matrix S [12]. After briefly reviewing the properties of S for symmetric scattering media, we shall derive the matrix elements for two classes of monodisperse ensembles. A monodisperse ensemble is one that has all its particles identical, in contradistinction to a polydisperse ensemble. We shall first derive S, using the Rayleigh-Gans-Born approximation, for a monodisperse ensemble of randomly oriented particles of arbitrary shape with a variable scalar refractive index $n(\vec{r})\,\delta_{ij}$. Using the same approximation, we shall secondly derive S for a monodisperse ensemble of randomly oriented, spherically shaped particles with a constant tensor refractive index n_{ij}. For an ensemble of this kind, we shall outline a procedure for obtaining a shape parameter γ for the constituent particles. We shall suggest that one may be able to modify this procedure to yield information for more general kinds of ensembles.

2. The Stokes Matrix for Symmetric Media

The experimental procedure for measuring the Stokes matrix elements has been presented elsewhere [13]. In this section, the well-known properties of the Stokes matrix are reviewed.

If one knows the scattering amplitude for a particular scattering process, one can obtain the Stokes matrix [14].

Consider an incident plane wave traveling in the +z direction. Let it be scattered by a particle located at the origin of our coordinate system. We are interested in determining the amplitude matrix of the outgoing spherical wave. This matrix is generally a function of the polar angle θ and the azimuthal angle ϕ. Because of the linearity of Maxwell's equations, one obtains:

$$\begin{pmatrix} E_{\parallel}^{sc} \\ E_{\perp}^{sc} \end{pmatrix} = \frac{e^{ikr}}{r} \begin{pmatrix} A_2(\theta,\phi) & A_3(\theta,\phi) \\ A_4(\theta,\phi) & A_1(\theta,\phi) \end{pmatrix} \begin{pmatrix} E_{\parallel}^{0} \\ E_{\perp}^{0} \end{pmatrix} \tag{1}$$

where $E_{\parallel,\perp}^{0}$ and $E_{\parallel,\perp}^{sc}$ are the components of the initial and final electric vectors measured parallel and perpendicular to the scattering plane. (the plane passing through the z-axis at an angle ϕ).

In the next section, we shall present a method for calculating the amplitude matrix. We shall confine our attention here to determining the Stokes matrix, given the amplitude matrix.

The elements of the Stokes vector (I,Q,U,V) are defined by

$I = \langle |E_{\parallel}|^2 + |E_{\perp}|^2 \rangle$, $Q = \langle |E_{\parallel}|^2 - |E_{\perp}|^2 \rangle$, $U = 2\langle \mathrm{Re}\ E_{\parallel}^{*} E_{\perp} \rangle$, and $V = 2\langle \mathrm{Im}\ E_{\parallel}^{*} E_{\perp} \rangle$. The brackets denote time averages. The Stokes matrix

is a 4×4 matrix that transforms the initial Stokes vector (I^0, Q^0, U^0, V^0) into the scattered Stokes vector $(I^{sc}, Q^{sc}, U^{sc}, V^{sc})$; i.e.,

$$\begin{pmatrix} I^{sc} \\ Q^{sc} \\ U^{sc} \\ V^{sc} \end{pmatrix} = \frac{S}{r^2} \begin{pmatrix} I^0 \\ Q^0 \\ U^0 \\ V^0 \end{pmatrix} . \tag{2}$$

The structure of S follows from Eqs. (1) and (2) using the definition of the Stokes vector:

$$S(\theta,\phi) = \begin{pmatrix} \frac{1}{2}(M_1+M_2+M_3+M_4) & \frac{1}{2}(M_2-M_3+M_4-M_1) & R_{23}+R_{41} & -I_{23}-I_{41} \\ \frac{1}{2}(M_2+M_3-M_4-M_1) & \frac{1}{2}(M_2-M_3-M_4+M_1) & R_{23}-R_{41} & -I_{23}+I_{41} \\ R_{24}+R_{31} & R_{24}-R_{31} & R_{21}+R_{34} & -I_{21}+I_{34} \\ I_{24}+I_{31} & I_{24}-I_{31} & I_{21}+I_{34} & R_{21}-R_{34} \end{pmatrix} \tag{3}$$

where $M_i \equiv |A_i|^2$, $I_{ij} \equiv \mathrm{Im}(A_i^* A_j)$, and $R_{ij} \equiv \mathrm{Re}(A_i^* A_j)$.

We shall be concerned with media composed, not of one particle in the scattering region as assumed above, but of many particles incoherently scattering the radiation. We shall assume media that are optically thin so that multiple scattering is negligible. For such media the composite Stokes matrix S^c is given by the sum of all the particles' Stokes matrices.

All the optical information about the medium contained in the scattered light is specified by the Stokes matrix. As originally demonstrated by Perrin [15], the imposition of various symmetry conditions simplifies the structure of S.

If one assumes that the scattering region remains invariant under reflection about any plane through its center, then R_{24}, I_{24}, R_{31}, I_{31}, R_{23}, I_{23}, R_{14}, and I_{14} vanish. If, additionally, the scattering region is isotropic and satisfies the conditions for optical reciprocity, then

$$S^c(\theta,\phi) = S^c(\theta) = \begin{pmatrix} a_1(\theta) & b_1(\theta) & 0 & 0 \\ b_1(\theta) & a_2(\theta) & 0 & 0 \\ 0 & 0 & a_3(\theta) & b_2(\theta) \\ 0 & 0 & -b_2(\theta) & a_4(\theta) \end{pmatrix} . \tag{4}$$

If, furthermore, we impose the condition that spherically symmetric, i.e., isotropic, particles are incoherently scattering the radiation, we find that:

$$a_1(\theta) = a_2(\theta), \qquad a_3(\theta) = a_4(\theta) \ . \tag{5}$$

If the spheres are identical, then the constraint

$$R(\theta) \equiv \frac{a_3(\theta)a_4(\theta) + b_2^2(\theta)}{a_1(\theta)a_2(\theta) - b_1^2(\theta)}$$

$$= \frac{a_3^2(\theta) + b_2^2(\theta)}{a_1^2(\theta) - b_1^2(\theta)} = 1, \tag{6}$$

is also satisfied. Equation (6) follows immediately from the property satisfied by the Stokes matrix elements for one particle (see Eq. (3)): $S_{11}(\theta,\phi)S_{22}(\theta,\phi) - S_{12}(\theta,\phi)S_{21}(\theta,\phi) = S_{33}(\theta,\phi)S_{44}(\theta,\phi) - S_{34}(\theta,\phi)S_{43}(\theta,\phi)$.

Therefore, if $a_1 \neq a_2$ or $a_3 \neq a_4$, as in the study of Holland and Gagne [16], one knows immediately that the scattering medium is composed of anisotropic particles. The converse of this statement need not be valid.

We shall now present the conventional formalism for deriving the amplitude matrix for the scattering of electromagnetic radiation by a single particle. We shall use the notation of Newton [17].

3. The Scattering Amplitude Matrix

In the absence of any scattering, the electric vector for a plane electromagnetic wave of unit amplitude traveling in the direction of its wave vector $\vec{k}$ ($|\vec{k}| = k$) may be represented at point $\vec{r}$ by:

$$\vec{E}(\vec{k},\nu,\vec{r}) = \vec{E}^0(\vec{k},\nu,\vec{r}) \equiv \vec{\chi}_\nu(\vec{k})e^{i\vec{k}\cdot\vec{r}}; \qquad \vec{k}\cdot\vec{\chi}_\nu(\vec{k}) = 0 \ , \tag{7}$$

where $\vec{\chi}_\nu(\vec{k})$ is the unit polarization vector of the incident wave. The time dependence has been suppressed. If a particle is then placed at the origin of the coordinate system, the electric vector is then modified by the scattering of the same incident wave:

$$\vec{E}(\vec{k},\nu,\vec{r}) = \vec{E}^0(\vec{k},\nu,\vec{r}) + \vec{E}^{sc}(\vec{k},\nu,\vec{r}), \tag{8}$$

where, asymptotically

$$\lim_{r \to \infty} \vec{E}^{sc}(\vec{k},\nu,\vec{r}) = \frac{e^{i\vec{k}\cdot\vec{r}}}{r} \sum_{\nu'=\parallel}^{\perp} \vec{\chi}_{\nu'}(\vec{k}')A(\vec{k}',\nu';\vec{k},\nu) \tag{9}$$

and, of course, via Eq. (7), $\vec{k}' \cdot \vec{\chi}_{\nu'}(\vec{k}') = 0$. Equation (9) states that the scattered wave is an outgoing spherical wave. The amplitude for the scattering from the incident direction $\vec{k}$ and polarization ν to a final direction $\vec{k}'$ and polarization ν' is given by $A(\vec{k}',\nu';\vec{k},\nu)$. One may choose ν and ν' to be polarization states parallel and perpendicular to the scattering plane, the plane normal to $\vec{k} \times \vec{k}'$.

In order to relate Eq. (9) to Eq. (1), we let the incident wave travel in the +z direction and look at the radiation scattered in the (θ,ϕ) direction. We must then have:

$$\vec{k} = k\hat{z}; \quad \vec{k}' = k(\sin\theta \cos\phi\, \hat{x} + \sin\theta \sin\phi\, \hat{y} + \cos\theta \hat{z}), \tag{10}$$

where $\hat{x},\hat{y},\hat{z}$ are unit vectors along the x,y,z axes. Since the scattering plane is now determined (being the plane containing the z-axis and oriented at an angle ϕ with respect to the +x-axis), the polarization vectors can also be determined:

$$\vec{\chi}_{\parallel}(\vec{k}) = \cos\phi\, \hat{x} + \sin\phi\, \hat{y}; \quad \vec{\chi}_{\parallel}(\vec{k}') = \cos\theta \cos\phi\, \hat{x} + \cos\theta \sin\phi\, \hat{y} - \sin\theta\, \hat{z};$$

$$\vec{\chi}_{\perp}(\vec{k}) = -\sin\phi\, \hat{x} + \cos\phi\, \hat{y}; \quad \vec{\chi}_{\perp}(\vec{k}') = -\sin\phi\, \hat{x} + \cos\phi\, \hat{y}\,. \tag{11}$$

We also can determine the elements of the scattering amplitude matrix of Eq. (1):

$$\begin{aligned} A_1(\theta,\phi) &= A(\vec{k}', \perp; \vec{k}, \perp); \quad A_2(\theta,\phi) = A(\vec{k}', \parallel; \vec{k}, \parallel); \\ A_3(\theta,\phi) &= A(\vec{k}', \parallel; \vec{k}, \perp); \quad A_4(\theta,\phi) = A(\vec{k}', \perp; \vec{k}, \parallel). \end{aligned} \tag{12}$$

By use of Maxwell's equations, the right-hand sides of (12) may be expressed as integrals over the volume V of the scattering particle:

$$A(\vec{k}',\nu';\vec{k},\nu) = \frac{k^2}{4\pi} \sum_{i,j=1}^{3} \int_V d^3r\, E_i^{0\,*}(\vec{k}',\nu',\vec{r}) p_{ij}(\vec{r}) E_j(\vec{k},\nu,\vec{r}), \tag{13}$$

$$p_{ij}(\vec{r}) = p_{ji}(\vec{r}) = (n^2(\vec{r}) - \underline{1})_{ij}, \quad [n^2(\vec{r})]_{ij} = \varepsilon_{ij}(\vec{r}) + \frac{4\pi i}{\omega} \sigma_{ij}(\vec{r}),$$

where $\underline{1}$ is the unit tensor, $\varepsilon_{ij}(\vec{r})$ and $\sigma_{ij}(\vec{r})$ are, respectively, the values of the dielectric constant tensor and conductivity tensor at point $\vec{r}$, and $\omega(=ck)$ is the angular frequency of the incident wave. The tensor $n_{ij}(\vec{r})$ is the refractive index tensor. We are assuming in Eq. (13) that the magnetic permeability μ of the scatterer is unity. The subscripts i and j refer to the coordinate axes. $\vec{E}(\vec{k},\nu,\vec{r})$ refers to the exact solution for the electric field vector as defined in Eq. (8). Equation (7) defines $\vec{E}^0(\vec{k}',\nu',\vec{r})$.

We shall approximate the exact solution for $\vec{E}(\vec{k},\nu,\vec{r})$ by substituting in its place the solution with no scattering, $\vec{E}^0(\vec{k},\nu,\vec{r})$:

$$A(\vec{k}',\nu';\vec{k},\nu) = \frac{k^2}{4\pi} \sum_{i,j=1}^{3} \int_V d^3r\ E_i^{0*}(\vec{k}',\nu',\vec{r}) p_{ij}(\vec{r}) E_j^0(\vec{k},\nu,\vec{r}). \qquad (14)$$

Equation (14) is the Rayleigh-Gans-Born (RGB) approximation [18] for the scattering amplitude and is expected to be valid when $|p_{ij}| \ll 1$ and $ka|p_{ij}| \ll 1$, where a is a typical dimension of the scatterer.

4. Applications of the RGB Approximation I: Variable Scalar Refractive Index

An isotropic or spherically symmetric particle has a scalar refractive index satisfying $n_{ij}(\vec{r}) = n(r)\delta_{ij}$. Water- or ice-coated spherical particles are examples of inhomogeneous isotropic particles found in the atmosphere. However, most aerosol particles are anisotropic.

We shall use the RGB approximation to study scattering of electromagnetic radiation by two classes of monodisperse ensembles of randomly oriented anisotropic particles.

First we shall treat the scattering by a monodisperse ensemble whose particles are defined by the refractive index $n_{ij}(\vec{r}) = n(\vec{r})\delta_{ij}$. Since this refractive index is generally not spherically symmetric, this definition applies to each particle in a certain orientation with respect to the coordinate axes. Plugging this refractive index into the RGB approximation, Eq. (14), yields:

$$A(\vec{k}',\nu';\vec{k},\nu) = \frac{k^2}{4\pi} \vec{\chi}_{\nu'}^{\dagger}(\vec{k}') \cdot \vec{\chi}_{\nu}(\vec{k}) \{ \int_V e^{i\Delta\vec{k}\cdot\vec{r}}\ p(\vec{r}) d^3r \}, \qquad (15)$$

where $\Delta\vec{k} = \vec{k} - \vec{k}'$ and $p(\vec{r}) = n^2(\vec{r}) - 1$. Using Eqs. (11) and (12), we obtain:

$$\begin{aligned} A_1(\theta,\phi) &= \frac{k^2}{4\pi} \int_V e^{i\Delta\vec{k}\cdot\vec{r}}\ p(\vec{r}) d^3r, \\ A_2(\theta,\phi) &= \frac{k^2}{4\pi} \{ \int_V e^{i\Delta\vec{k}\cdot\vec{r}}\ p(\vec{r}) d^3r \} \cos\theta, \qquad (16) \\ A_3(\theta,\phi) &= A_4(\theta,\phi) = 0 . \end{aligned}$$

The Stokes matrix for the scattering by one particle of the ensemble follows using Eq. (3):

$$S(\theta,\phi) = \frac{k^4}{32\pi^2}\left|\int_V e^{i\Delta\vec{k}\cdot\vec{r}}p(\vec{r})d^3r\right|^2 \begin{pmatrix} 1+\cos^2\theta & \cos^2\theta-1 & 0 & 0 \\ \cos^2\theta-1 & 1+\cos^2\theta & 0 & 0 \\ 0 & 0 & 2\cos\theta & 0 \\ 0 & 0 & 0 & 2\cos\theta \end{pmatrix} \tag{17}$$

To obtain the composite Stokes matrix for the ensemble, S^c, we sum all of the particles' Stokes matrices. If there are N identical randomly oriented particles, this sum is equivalent to averaging over all possible orientations of $\Delta\vec{k}$. The composite Stokes matrix is therefore given by:

$$S^c(\theta,\phi) = S^c(\theta) = f(\theta) \begin{pmatrix} 1+\cos^2\theta & \cos^2\theta-1 & 0 & 0 \\ \cos^2\theta-1 & 1+\cos^2\theta & 0 & 0 \\ 0 & 0 & 2\cos\theta & 0 \\ 0 & 0 & 0 & 2\cos\theta \end{pmatrix} \tag{18}$$

where

$$f(\theta) = \frac{N}{4\pi}\left\{\frac{k^4}{32\pi^2}\int d\Omega_{\hat{\Delta k}}\left|\int_V e^{i\Delta\vec{k}\cdot\vec{r}}p(\vec{r})d^3r\right|^2\right\} \tag{19}$$

and $\int d\Omega_{\Delta k}$ = integration over solid angle of $\Delta\vec{k}$. To simplify the right-hand side of Eq. (19), we use the well-known plane wave decomposition:

$$e^{i\Delta\vec{k}\cdot\vec{r}} = 4\pi\sum_{\ell=0}^{\infty}\sum_{m=-\ell}^{\ell}(i)^\ell j_\ell(|\Delta\vec{k}|r)Y_\ell^m(\hat{r})Y_\ell^{m*}(\hat{\Delta k}),$$

where the Y_ℓ^m are the spherical harmonics, j_ℓ are the spherical Bessel functions of the first kind, and $\hat{}$ denotes unit vectors. In our case $|\Delta\vec{k}| = 2k\sin\frac{1}{2}\theta$, where θ is the scattering angle. We then find that:

$$f(\theta) = \frac{N}{4\pi}\left(\frac{k^4}{32\pi^2}\right)\iint d^3r\, d^3r' p(\vec{r})p(\vec{r}')\int d\Omega_{\hat{\Delta k}} e^{i\Delta\vec{k}\cdot\vec{r}}e^{-i\Delta\vec{k}\cdot\vec{r}'}$$

$$= N\frac{k^4}{8\pi}\sum_{\substack{\ell,m\\ \ell',m'}}(i)^\ell(-i)^{\ell'}\iint d^3r d^3r' p(\vec{r})p(\vec{r}')j_\ell(2kr\sin\tfrac{1}{2}\theta)j_{\ell'}(2kr'\sin\tfrac{1}{2}\theta)$$

$$\cdot\, Y_\ell^m(\hat{r})Y_{\ell'}^{m'*}(\hat{r}')\int d\Omega_{\hat{\Delta k}}\, Y_\ell^{m*}(\hat{\Delta k})Y_{\ell'}^{m'}(\hat{\Delta k}) .$$

The integral over $d\Omega_{\hat{\Delta k}}$ reduces to $\delta_{\ell\ell'}\delta_{mm'}$. Therefore, we finally obtain:

$$f(\theta) = N\frac{k^4}{8\pi} \sum_{\ell,m} \left| \int_V d^3r' p(\vec{r}') j_\ell(2kr' \sin\tfrac{1}{2}\theta) Y_\ell^m(\hat{r}') \right|^2 . \tag{20}$$

Note that the θ in the argument of the spherical Bessel functions is not an integration variable; it is the fixed scattering angle determined by the magnitude of $\Delta\vec{k}$.

Unlike Eq. (19), Eq. (20) lends itself to physical interpretation. For example, if we are dealing with spherically symmetric inhomogeneous particles, i.e., $p(\vec{r}') = p(r')$, then only the $\ell = 0$, $m = 0$ term contributes:

$$f(\theta) = \frac{Nk^4}{2} \left| \int_V r'^2 p(r') j_0(2kr' \sin\tfrac{1}{2}\theta) dr' \right|^2 . \tag{21}$$

Furthermore, if $p(r') = n^2 - 1$ for $r' < a$ and $p(r') = 0$ for $r' > a$, then we may perform the integration to obtain the well-known result for incoherent scattering by N identical homogeneous spheres:

$$f(\theta) = \frac{Nk^2a^4}{8} (n^2-1)^2 \frac{j_1^2(2ka \sin\frac{1}{2}\theta)}{\sin^2 \frac{1}{2}\theta} . \tag{22}$$

Expanding Eq. (22) in powers of ka and keeping only the lowest order term in ka, we obtain the Rayleigh scattering formula for $f(\theta)$:

$$f(\theta) = \frac{Nk^4a^6}{18} (n^2-1)^2 . \tag{23}$$

The terms in Eq. (20) with $\ell \neq 0$ reflect the anisotropy or departure from spherical symmetry of the individual scattering particles.

If each particle of our monodisperse ensemble has an axis of rotational symmetry, we then can orient our coordinate system so that $p(\vec{r}')$ in Eq. (20) has a rotational symmetry axis pointing along the z-axis; i.e., $p(\vec{r}') = p(r',\mu')$. Only the $m = 0$ terms will then contribute to the right-hand side of Eq. (20), yielding:

$$f(\theta) = \frac{Nk^4}{8} \sum_\ell (2\ell+1) \left| \iint_V dr' d\mu' r'^2 p(r',\mu') j_\ell(2kr' \sin\tfrac{1}{2}\theta) P_\ell(\mu') \right|^2 , \tag{24}$$

where $P_\ell(\mu')$ is the ℓ^{th} Legendre polynomial. If, in Eq. (24), $p(r',\mu') = p(r',-\mu')$, then only the even ℓ terms can contribute to $f(\theta)$.

Using Eq. (24), one can reproduce the results summarized by Van de Hulst for the scattering of electromagnetic radiation by monodisperse ensembles of randomly oriented, infinitely thin homogeneous rods or disks [19]. In the case of rods of length L, one sets

$$p(r',\mu') \propto (n^2-1)\,\frac{\delta(\mu'^2-1)}{r'^2} \quad \text{for} \quad 0 \leq r' \leq \frac{L}{2}\ , \quad -1 \leq \mu' \leq 1, \text{ and}$$

$p(r',\mu') = 0$ elsewhere. In the case of disks of radius a, one sets

$$p(r',\mu') \propto (n^2-1)\,\frac{\delta(\mu')}{r'} \quad \text{for} \quad 0 \leq r' \leq a, \quad -1 \leq \mu' \leq 1, \text{ and} \quad p(r',\mu') = 0$$

elsewhere. The functions $\delta(\mu'^2-1)$ and $\delta(\mu')$ are Dirac delta functions.

To summarize: in this section we have derived the Stokes matrix, Eq. (18), for a monodisperse ensemble of randomly oriented anisotropic particles defined by the refractive index $n_{ij}(\vec{r}) = n(\vec{r})\delta_{ij}$. We have derived Eq. (20) without any additional assumptions. We have noted that if the particles have an axis of rotational symmetry, then Eq. (20) reduces to Eq. (24).

We conclude this section by generalizing Eq. (20) to the case of a polydisperse ensemble of randomly oriented particles. If we have m kinds of particles defined by $p_i(\vec{r})$, $i = 1,2,\ldots,m$, and if there are N_i particles of the i^{th} kind, then for the polydisperse ensemble, $f(\theta)$ is given by:

$$f(\theta) = \frac{k^4}{8\pi} \sum_{i=1}^{m} N_i \sum_{\ell,m} \left| \int d^3r' p_i(\vec{r}') j_\ell(2kr' \sin\tfrac{1}{2}\theta) Y_\ell^m(\hat{r}') \right|^2 . \qquad (25)$$

5. Applications of the RGB Approximation II: Constant Tensor Refractive Index

In this section, we shall use the RGB approximation, Eq. (14), to compute the composite Stokes matrix for a monodisperse ensemble of randomly oriented anisotropic particles defined by the refractive index $n_{ij}(\vec{r}) = n_{ji}(\vec{r}) = n_{ij}$ for $r < a$ and $n_{ij}(\vec{r}) = \delta_{ij}$ for $r > a$. This refractive index implies that $p_{ij}(\vec{r}) = p_{ji}(\vec{r}) = p_{ij}$ for $r < a$ and $p_{ij} = 0$ for $r > a$. This definition applies to each particle for a certain orientation with respect to the coordinate axes. As the orientation of the particle changes, the values of the tensor components p_{ij} vary in a well-known fashion [20].

The amplitude for the scattering by a single particle in a fixed orientation is then

$$A(\vec{k}',\nu';\vec{k},\nu) = \frac{k^2}{4\pi} \sum_{i,j=1}^{3} \chi^*_{\nu',i}(\vec{k}')p_{ij}\,\chi_{\nu,j}(\vec{k}) \int_{r<a} d^3r\, e^{i\Delta\vec{k}\cdot\vec{r}}$$

$$= \frac{1}{2}\,ka^2\,\frac{j_1(2ka\,\sin\frac{1}{2}\theta)}{\sin\frac{1}{2}\,\theta}\;\chi^*_{\nu',i}(\vec{k}')p_{ij}\,\chi_{\nu,j}(\vec{k})$$

$$\equiv g(\theta)\chi^*_{\nu',i}(\vec{k}')p_{ij}\,\chi_{\nu,j}(\vec{k})\ .$$

Using Eqs. (11) and (12), we find that:

$$\begin{aligned} A_1(\theta,\ \phi=0) &= g(\theta)p_{22}, \\ A_2(\theta,\ \phi=0) &= g(\theta)(\cos\theta\ p_{11} - \sin\theta\ p_{31}), \\ A_3(\theta,\ \phi=0) &= g(\theta)(\cos\theta\ p_{12} - \sin\theta\ p_{32}), \\ A_4(\theta,\ \phi=0) &= g(\theta)p_{21}\ . \end{aligned} \tag{26}$$

One may compute the composite Stokes matrix for an ensemble of N of these particles randomly oriented [21]:

$$S^c(\theta,\phi) = \frac{N}{2}\,g^2(\theta)\beta \begin{pmatrix} 2(1+\gamma)+(\gamma-1)\sin^2\theta & (\gamma-1)\sin^2\theta & 0 & 0 \\ (\gamma-1)\sin^2\theta & (1-\gamma)(1+\cos^2\theta) & 0 & 0 \\ 0 & 0 & 2(1-\gamma)\cos\theta & 0 \\ 0 & 0 & 0 & 2(1-3\gamma)\cos\theta \end{pmatrix} \tag{27}$$

Note that, as in Eq. (18), $S^c(\theta,\phi)$ is ϕ-independent.

The parameters β and γ define those measurable quantities of this monodisperse ensemble that reflect the optical anisotropy of the particles. If p_1, p_2, and p_3 are the eigenvalues of the matrix $\{p_{ij}\}$, then

$$\begin{aligned} \beta &= \frac{3}{15}\,(p_1^2 + p_2^2 + p_3^2) + \frac{2}{15}(p_1p_2 + p_2p_3 + p_3p_1), \\ \gamma &= \frac{1}{15\beta}\,[(p_1^2 + p_2^2 + p_3^2) - (p_1p_2 + p_1p_3 + p_3p_1)]. \end{aligned} \tag{28}$$

The physical meaning of these eigenvalues is made transparent by noting

that $(p_i+1)^{1/2}$ for $i = 1,2,3$ are the lengths of the principal axes of the particle's Fresnel ellipsoid [22]. If the ellipsoid reduces to a sphere, as in the case of isotropic particles, then $p_1 = p_2 = p_3$ so that $\gamma = 0$. In this case, Eq. (27) must and does yield the matrix given by Eqs. (18) and (22).

When $\gamma = 0$ in Eq. (27), we obtain $S_{11}^c = S_{22}^c$ and $S_{33}^c = S_{44}^c$, which, as we have noted earlier, is a necessary condition for Stokes matrices of isotropic particles.

One should note that if $g(\theta)$ is expanded in powers of ka and only the lowest order term is kept, then Eq. (27) gives the usual result for scattering by randomly oriented anisotropic dipolar particles [23].

One may obtain the Rayleigh result, Eqs. (18) and (23), from Eq. (27), by keeping only the lowest order term in ka in the power series expansion of $g(\theta)$ *and* by choosing $\gamma = 0$.

The results of this section may be generalized.

If one extends the derivation of the composite Stokes matrix presented in this section to the case of particles having the more general tensor refractive index $n_{ij}(\vec{r}) = n_{ji}(\vec{r}) = F(r)n_{ij}$, $r < a$ (where $F(r)$ is an arbitrary function depending solely on $|\vec{r}|$), one finds that $g(\theta)$ is no longer proportional to $\dfrac{j_1(2ka \sin\frac{1}{2}\theta)}{\sin\frac{1}{2}\theta}$; otherwise the composite Stokes matrix is unaltered. Even though the size of the Fresnel ellipsoid for this refractive index $F(r)n_{ij}$ is a function of r, the shape of the ellipsoid is constant throughout the particle. The parameter γ remains the shape parameter of the Fresnel ellipsoid; e.g., $\gamma = 0$ implies isotropy.

For the even more general tensor refractive index $n_{ij}(\vec{r}) = n_{ji}(\vec{r}) = n_{ij}(r)$, $r < a$, the parameters β and γ become θ-dependent. In this latter (rather artificial) case, the size and shape of the Fresnel ellipsoid of $n_{ij}(r)$ are functions of r.

Finally, as does Eq. (20), Eq. (27) admits generalization to the case of polydisperse ensembles of randomly oriented particles with tensor refractive indices.

6. Summary: Implications for Future Research

Crucial for the understanding of the effects of real aerosols in any radiative transfer problem is a knowledge of features that distinguish electromagnetic radiation scattered by real aerosols from radiation scattered by an ensemble of homogeneous spheres. Such knowledge is essential for understanding the polarization of radiation scattered by real aerosols, since polarization is very sensitive to the shape and structure of the scatterer.

Using the RGB approximation, we have studied above the departures from Mie scattering, i.e., the scattering by homogeneous spheres. We have derived the Stokes matrices for two classes of ensembles of randomly oriented anisotropic particles and have discussed possible generalizations.

If the elements of a Stokes matrix do not satisfy Eq. (5), we know that anisotropic particles are scattering the radiation. If the elements do not satisfy Eq. (6), we know that the scattering particles do not constitute a monodisperse ensemble of spheres. These conditions are well known. The violation of Eqs. (5) and (6) should be studied as a function of particle and ensemble structure. For example, computer experiments could be performed on polydisperse ensembles of homogeneous spheres, using Mie theory, to isolate the effects of polydispersity upon $R(\theta)$ as defined by Eq. (6):

$$R(\theta) \equiv \frac{S_{33}^c(\theta)S_{44}^c(\theta) = S_{34}^c(\theta)S_{43}^c(\theta)}{S_{11}^c(\theta)S_{22}^c(\theta) - S_{12}^c(\theta)S_{21}^c(\theta)} \quad .$$

Perhaps polydispersity effects are significant at some scattering angles and are always negligible at others. One then may be able to disentangle the effects of particle shape and structure from the effects of polydispersity when analyzing $R(\theta)$.

For a monodisperse ensemble of anisotropic particles with constant tensor refractive index, we note from Eq. (27) that in the RGB approximation,

$$R(\theta) = \frac{(1-3\gamma)\cos^2\theta}{\gamma + \cos^2\theta} \quad . \tag{29}$$

For this kind of ensemble, $R(\theta)$ is a function of only θ and γ. Using Eq. (28), we see that $0 \leq \gamma \leq \frac{1}{3}$. For Fresnel spheres ($p_1 = p_2 = p_3$), $\gamma = 0$ and $R(\theta) = 1$. For Fresnel "needles" ($p_1 \neq 0$, $p_2 = p_3 = 0$), $\gamma = \frac{1}{3}$ and $R(\theta) = 0$. At $\theta = 0°$ or $\theta = 180°$, $R = \frac{1-3\gamma}{1+\gamma}$. Finally, $R = 0$ at $\theta = 90°$ for $\gamma \neq 0$.

For a monodisperse ensemble of anisotropic particles with scalar refractive index $n(\vec{r})\delta_{ij}$, we note from Eq. (18) that $R(\theta) = 1$ in the RGB approximation. (Remember that $R(\theta) = 1$ is a necessary but insufficient condition that the scatterers be isotropic.) If we relax the RGB constraint that $n^2(\vec{r}) - 1$ be small, we must also consider terms of second order in $n^2(\vec{r}) - 1$ in the scattering amplitude. Then the ratio $R(\theta)$ is no longer unity. For example, consider the case of scattering by a monodisperse ensemble of randomly oriented homogeneous ellipsoids. In the quasi-static limit $ka << 1$, we may expand the components p_1, p_2, and p_3, of the diagonalized polarization tensor in powers of $n^2 - 1$. We then find that these components differ from each other in the second order term in $n^2 - 1$ [24]. Equation (30) then might be qualitatively a parameterization for $R(\theta)$, with γ now related to the particles' geometric shape.

(Remember that Eq. (30) was originally derived not for particles with ellipsoidal boundaries, but for particles with $n_{ij}(\vec{r}) = n_{ij}$ for $r < a$ and $n_{ij}(\vec{r}) = 1$ otherwise.)

This admittedly heuristic and qualitative discussion shows the need for further analysis. Limitations upon the validity of various theoretical models should be examined by laboratory studies of simple monodisperse and polydisperse ensembles of particles whose size, shape and structure are carefully controlled. Further theoretical work must be done in order to understand and construct scattering models where the RGB approximation is inappropriate and Mie theory fails. First, one must improve upon the plane wave assumption $\vec{E} = \vec{E}_0$ utilized in obtaining the RGB approximation, Eq. (14). Finding the solution for scattering by realistic aerosols represents a formidable challenge.

References

1. J. Tyndall, *Phil. Mag.*, 37, 384; 38, 156 (1869).

2. J. W. Strutt (Lord Rayleigh), *Nature*, 3, 234, 264, 265 (1871); *Phil. Mag.*, 41, 107, 274, 447 (1871).

3. M. Kerker, *The Scattering of Light and Other Electromagnetic Radiation* (Academic Press, New York, 1969).

4. J. Mayo Greenberg, "Interstellar Grains," in *Nebulae and Interstellar Matter*, ed. by B. M. Middlehurst and L. H. Aller (University of Chicago Press, Chicago, 1968).

5. S. I. Rasool and S. H. Schneider, *Science*, 173, 138 (1971).

6. J. E. Hansen, *J. Atmos. Sci.*, 28, 1400 (1971); Z. Sekera, Science Progress No. 179, 479 (1957); Z. Sekera, *Icarus*, 6, 348 (1967); K. L. Coulson, *J. Quant. Spectrosc. Radiat. Transfer*, 11, 739 (1971); *Man's Impact on the Global Environment: Assessment and Recommendations for Action*, A report of the Study of Critical Environmental Problems (SCEP), (The MIT Press, Cambridge, Massachusetts, 1970); *Inadvertent Climate Modification*, A Report of the Study of Man's Impact on Climate (SMIC), (The MIT Press, Cambridge, Massachusetts, 1970); *Remote Measurement of Pollution*, prepared by NASA Langley Research Center (Scientific and Technical Information Office, NASA, Washington, D.C., 1971).

7. D. Deirmendjian, *Electromagnetic Scattering on Spherical Polydispersions* (Elsevier, New York, 1969).

8. G. Mie, *Ann. Physik*, 25, 377 (1908).

9. J. E. Hansen, *J. Atmos. Sci.*, 28, 1400 (1971).

10. A. C. Holland and G. Gagne, *Appl. Opt.*, 9, 1113 (1970).

11. Z. Sekera, *Icarus*, 6, 348 (1967).

12. G. Stokes, *Trans. Cambridge Phil. Soc.*, 9, 399 (1852).

13. Z. Sekera, "Polarization of Skylight," in *Handbuch der Physik*, Vol. 48, ed. by J. Bartels (Springer-Verlag, Berlin, 1957).

14. H. C. Van de Hulst, *Light Scattering by Small Particles* (John Wiley and Sons, Inc., New York, 1957).

15. F. Perrin, *J. Chem. Phys.*, 10, 415 (1942).

16. A. C. Holland and G. Gagne, *Appl. Opt.*, 9, 1113 (1970).

17. Roger G. Newton, *Scattering Theory of Waves and Particles*, (McGraw-Hill Book Co., New York, 1966).

18. J. W. Strutt (Lord Rayleigh), *Phil. Mag.*, 12, 81 (1881); R. Gans, *Ann. Physik*, 76, 29 (1925); M. Born, *Zeits. f. Physik*, 38, 803 (1926).

19. H. C. Van de Hulst, *Light Scattering by Small Particles* (John Wiley and Sons, Inc., New York, 1957).

20. *Ibid.* See also S. Chandrasekhar, *Radiative Transfer* (Dover Publications, Inc., New York, 1960).

21. *Ibid.*

22. M. Born and E. Wolf, *Principles of Optics* (Pergamon Press, Oxford, 1970).

23. F. Perrin, *J. Chem. Phys.*, 10, 415 (1942).

24. J. A. Stratton, *Electromagnetic Theory* (McGraw-Hill Book Co., New York, 1941). See also H. C. Van de Hulst, *Light Scattering by Small Particles* (John Wiley and Sons, Inc., New York, 1957).